AD-A094 124 FEDERAL AVIATION ADMINISTRATION TECHNICAL CENTER ATL--ETC F/G 17/9
DISCRETE ADDRESS BEACON SYSTEM (DABS) RECEIVER AND AIR TRAFFIC --ETC(U)
DEC 80 L H BAKER

UNCLASSIFIED FAA-CT-80-11 FAA-RD-80-75 NL

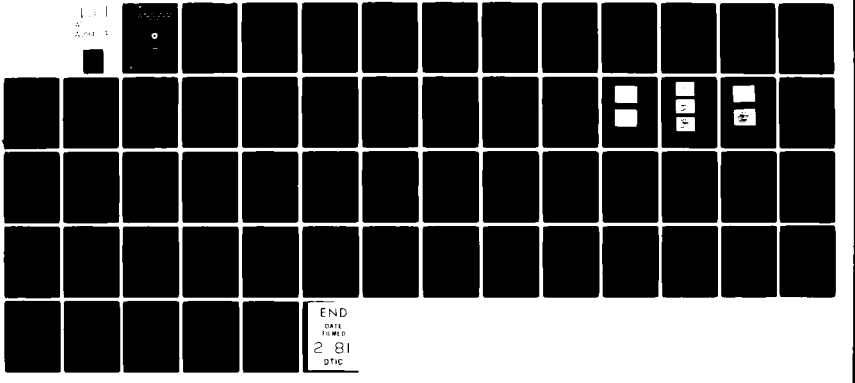

END
DATE FILMED
2 81
DTIC

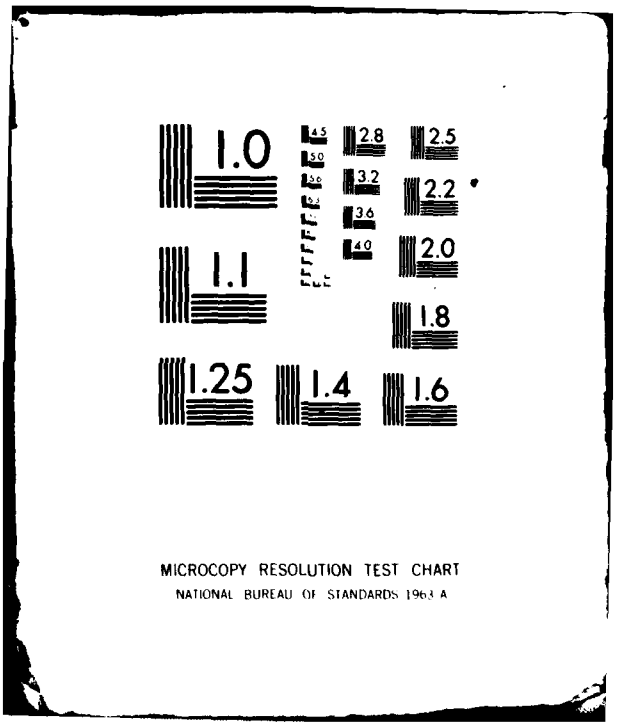
1.0
1.1
1.25
1.4
1.6
1.8
2.0
2.2
2.5
2.8
3.2
3.6
4.0
4.5
5.0
5.6
MICROCOPY RESOLUTION TEST CHART
NATIONAL BUREAU OF STANDARDS 1963 A

Report No. FAA-RD-80-75
FAA-CT-80-11

LEVEL II

DISCRETE ADDRESS BEACON SYSTEM (DABS) RECEIVER AND AIR TRAFFIC CONTROL RADAR BEACON SYSTEM (ATCRBS) AND DABS PROCESSOR SUBSYSTEM TESTS

Leonard H. Baker

FEDERAL AVIATION ADMINISTRATION TECHNICAL CENTER
Atlantic City Airport, New Jersey 08405

FINAL REPORT. Feb-Dec 79,

DEC 80

59

Prepared for

U. S. DEPARTMENT OF TRANSPORTATION
FEDERAL AVIATION ADMINISTRATION
Systems Research & Development Service
Washington, D. C. 20590

411863

81 1 26 047

NOTICE

This document is disseminated under the sponsorship of the Department of Transportation in the interest of *information exchange.* The United States Government assumes no liability for the contents or use thereof.

The United States Government does not endorse products or manufacturers. Trade or manufacturer's names appear herein solely because they are considered essential to the object of this report.

Technical Report Documentation Page

1. Report No.	2. Government Accession No.	3. Recipient's Catalog No.
FAA-RD-80-75	AD-A094124	

4. Title and Subtitle	5. Report Date
DISCRETE ADDRESS BEACON SYSTEM (DABS) RECEIVER AND AIR TRAFFIC CONTROL RADAR BEACON SYSTEM (ATCRBS) AND DABS PROCESSOR SUBSYSTEM TESTS	December 1980
	6. Performing Organization Code
7. Author(s)	8. Performing Organization Report No.
Leonard H. Baker	FAA-CT-80-11
9. Performing Organization Name and Address	10. Work Unit No. (TRAIS)
Federal Aviation Administration Technical Center Atlantic City Airport, New Jersey 08405	11. Contract or Grant No. 034-241-510
	13. Type of Report and Period Covered
12. Sponsoring Agency Name and Address	Final Feb. 1979 - Dec. 1979
U.S. Department of Transportation Federal Aviation Administration Systems Research and Development Service Washington, D.C. 20590	14. Sponsoring Agency Code

15. Supplementary Notes

16. Abstract

This report describes the subsystem interrogator and processor tests conducted by the Federal Aviation Administration (FAA) Technical Center on the engineering laboratory model of the Discrete Address Beacon System (DABS). These tests were conducted to determine the performance of the multichannel receiver and the Air Traffic Control Radar Beacon System (ATCRBS) and DABS processors. These performance test results supplement the functional subsystem testing performed by Texas Instruments, Incorporated during the factory tests.

The results of the receiver tests were used to determine the operating parameters and performance of the monopulse receiver and the operating characteristics of the video quantizer. The ATCRBS reply processor tests identified the static performance and characteristics of the variable parameters in this unit. The DABS reply processor tests defined the performance of the critical elements in the DABS processor. These elements were the video digitizer, the message bit and monopulse processing, and the error detection and correction. Identification and optimization of the characteristics of the variable parameters of this unit were determined. It was concluded that the subsystems tested met the requirements specified in the DABS engineering requirement (ER) FAA-ER-240-26.

17. Key Words	18. Distribution Statement
Beacon Data Processing Systems Data Transmission DABS	Document is available to the U.S. public through the National Technical Information Service, Springfield, Virginia 22161

19. Security Classif. (of this report)	20. Security Classif. (of this page)	21. No. of Pages	22. Price
Unclassified	Unclassified	59	

Form DOT F 1700.7 (8-72) Reproduction of completed page authorized

TABLE OF CONTENTS

LIST OF ILLUSTRATIONS

LIST OF ILLUSTRATIONS (Continued)

INTRODUCTION

OBJECTIVE.

The objective of these tests was to measure the performance characteristics of several functions within the interrogator and processor (I&P) subsystems of the Discrete Address Beacon System (DABS) engineering laboratory model. Using controlled inputs, the tests were designed to establish the best operating value for field adaptable parameters. The specific subsystems tested were: (1) the multichannel monopulse receiver and video pulse quantizer, (2) the Air Traffic Control Radar Beacon System (ATCRBS) hardware reply processor, and (3) the DABS hardware reply processor.

BACKGROUND.

The DABS has been designed as an evolutionary replacement for the ATCRBS to provide the enhanced surveillance and communications capability required for air traffic control (ATC) in the 1980's and 1990's. Compatibility with the ATCRBS has been emphasized to permit an extended and economical transition.

The requirement for the development of the DABS was identified in the 1969 Department of Transportation Air Traffic Control Advisory Committee (ATCAC) Study. The first phase of DABS development consisted of a feasibility study and validation of the DABS concept. This study was conducted by the Massachusetts Institute of Technology (MIT) Lincoln Laboratory. After successfully demonstrating the feasibility of the DABS concept, engineering requirement (ER) FAA-ER-240-26 was prepared by Lincoln Laboratory for the development of three single-channel DABS sensors which could operate as a network and interface with en route and terminal ATC facilities.

Texas Instruments (TI), Incorporated was awarded a contract to fabricate the three engineering laboratory models of the DABS sensor. They are installed at the Federal Aviation Administration (FAA) Technical Center and Clementon and Elwood, New Jersey. After completing factory acceptance tests, the sensors were delivered to the three sites where they were installed and subjected to field acceptance tests. Upon completion of the field acceptance tests, the performance tests outlined in Report No. FAA-NA-79-151, "DABS Single Sensor Performance Test Plan," were initiated using the Technical Center's sensor.

The I&P tests, conducted by TI at the factory, were developed to identify specific responses of hardware circuits for test pulse inputs. The performance tests, conducted by the Technical Center, defined subsystem performance by simulating actual pulse replies and interference expected in an ATCRBS/DABS environment.

DESCRIPTION OF EQUIPMENT

DABS MULTICHANNEL RECEIVER.

The multichannel receiver processes radiofrequency (RF) signals received from the DABS sensor antenna. The multichannel receiver outputs video and quantizer (two-level) video signals to the DABS and the ATCRBS reply processors. Quantized two-level signals, quantized sum ATCRBS (QΣA), quantized sum DABS (QΣD), quantized side-lobe suppression ATCRBS (QSLSA), and quantized side-lobe suppression DABS (QSLSD) are output by the receiver. These indicate the source of the input signal to the processor; either a main beam or a side lobe, and either a DABS or ATCRBS signal.

Quantized levels for the quantized sum positive slope (QΣPS) and the quantized sum negative slope (QΣNS) signals indicate when pulse slope level are exceeded. The receiver outputs an

analog signal which approximates the ratio difference/sum (Δ/Σ) from which the reply monopulse value is derived. The receiver uses 12 site-dependent adjustable levels to reduce: (1) low-level multipath signals, (2) close-in false targets due to reflections, and (3) noise detection. A threshold omnilevel (T_Ω) functions as amplitude-received side-lobe suppression. A threshold difference level (T_Δ) is used in conjunction with T_Ω to eliminate detection of pulses outside the main beam.

ATCRBS REPLY PROCESSOR.

Quantized video reply pulses from the receiver are applied through a buffer and multiplexor, located in the DABS reply processor, to the ATCRBS reply processor. Simultaneously, monopulse video from the receiver is applied to an analog-to-digital (A/D) converter. The ATCRBS reply processor converts the quantizer video into digital data. Target range is determined by measuring the time from the start of a predetermined acceptance window to the first reply pulse. An ATCRBS convert signal is applied to the A/D converter to output an 8-bit word representing the monopulse video input data from the receiver. The data are sampled once for each pulse in the ATCRBS reply. The samples are averaged by the reply processor to develop a monopulse estimate for each declared ATCRBS reply. The data detected and decoded by the processor are assembled into a report providing an estimate of target range, azimuth, code, and code pulse confidence. Also identified is the occurrence of overlapping, false, or garbled ATCRBS replies. The data are routed to the ATCRBS reply-to-reply correlator computer. All replies received from an aircraft during one antenna scan are then combined into a single target report.

DABS REPLY PROCESSOR.

The DABS reply processor operates on the receiver output from which it detects and decodes DABS All-Call and roll-call replies. It also generates an estimate of the target range and azimuth for each detected reply. Monopulse video from the receiver is converted into a serial data stream. DABS replies are detected on the basis of a four-pulse preamble preceding the reply data block. During interrogation, the processor is supplied with a listening window and an address by the channel management function. The received data stream is compared to the listening window and expected DABS address. If a reply with no error is detected, the message is assumed to be correct and output for surveillance processing. If an error is detected in either an All-Call or roll-call reply, an attempt is made to locate and correct it. If successful, the message is sent to the computer; if not, a decode fail is indicated.

AIRCRAFT REPLY AND INTERFERENCE ENVIRONMENT SIMULATOR (ARIES).

The ARIES was designed by Lincoln Laboratory to simulate DABS/ATCRBS target replies, ATCRBS fruit replies, communication (Comm) messages, and radar data. The interrogation interface between the sensor and the ARIES was at the RF level; the replies generated by the ARIES were available to the DABS at the receiver intermediate frequency (IF) level. Radar interface was accomplished via the DABS communication subsystem, as normally accomplished for radar. Various traffic samples were selected to test DABS under air traffic environments anticipated through 1995. Several different scenarios were generated for repeated playback through the ARIES. The scenarios were run and rerun with a variety of target and environment parameters.

Along with the simulated traffic, the ARIES generated a simulated fruit environment. The arrival times of fruit replies were not based on the traffic model. To do this would also require modeling the nearby interrogators that cause these interfering replies to be generated. Instead, fruit was modeled

as a random process with Poisson statistics. The operator can control the average fruit rate by setting parameters in a file on the system disk.

ARIES is capable of generating ATCRBS fruit replies at rates up to approximately 50,000 per second. These high rates were required to test the performance of the DABS sensor's reply processing circuitry at the interference levels at which it is capable of operating.

For both the simulated transponder (controlled) replies and fruit replies, the ARIES provides the necessary signals to accurately simulate the monopulse off-boresight angle. Also, an omnidirectional signal was provided so that side-lobe replies could be simulated. These signals were connected to the DABS sensor via an interface dedicated to the ARIES. The sensor added these signals to similar signals from the sensor's antenna. This allowed a simulated environment to be superimposed on a live environment.

A maximum of 400 targets was simulated by the ARIES. Any mix of DABS and ATCRBS targets was possible. In addition to the overall limitation on the number of targets, there were limitations on the number of targets bunched in azimuth. The ARIES was capable of generating the number of bunched targets specified for the DABS sensor, which are:

1. Fifty aircraft in an 11.25° sector for not more than eight consecutive sectors.

2. Twelve aircraft in a 1.0° azimuth wedge for up to four contiguous wedges.

In addition to the beacon data, the ARIES provided simulated digitized radar data in the output format of the common digitizer (CD). The radar targets correspond to the simulated beacon targets. The reported coordinates were those seen by a primary radar whose antenna rotated with the beacon antenna about the same axis. The ARIES operator can control the radar reply probability by setting parameters in file on the system disk.

The ARIES equipment consisted of interrogation receiving circuitry, reply generation circuitry, and a computer with associated peripheral equipment to control the system. This equipment was housed in two standard racks. A complete description of the ARIES is contained in Report No. FAA-RD-78-96.

TEST TARGET GENERATOR (TTG).

The TTG is a unit of special test equipment used to generate highly accurate digital pulse responses for input to the reply processor. It can be used in a secondary mode of operation to simulate DABS and ATCRBS replies to support IF/RF tests of the processor hardware. Both the digital and secondary mode of operation are used extensively in measuring the performance of the hardware processors.

The TTG essentially consists of two memories and a controller. Test scenarios and data blocks are read into the TTG via a card reader and stored in memory. The controller is used to control the input of data and synchronize the output with the DABS modulator control unit (MCU) listening windows.

RADIOFREQUENCY TEST UNIT (RFTU).

The RFTU is used to interface the digital output from the test target generator to the RF input of the DABS sensor. Three RF outputs provide the sum (Σ), difference (Δ), and omni (Ω) signals. The RFTU has the capability of adjusting the phase relationship of the Σ to Δ signals and the setting of RF attenuators to control output levels.

METHOD OF APPROACH

Test and evaluation (T&E) of the DABS multichannel receiver, the ATCRBS reply processor, and the DABS reply processor were divided into three phases. The first phase determined performance measurements of the DABS multichannel receiver. The results are presented in the sequence of the individual tests defined. Each test procedure was followed by test data and/or plotted results defining the appropriate performance.

The second phase of tests was designed to determine the performance of the ATCRBS reply processor as a function of site adaptable parameters. Optimization of each parameter resulted from these tests. The test target generator was the source of reply target information for these tests.

The third phase of testing determined the overall performance of the DABS reply processor. The performance was measured using various input signal conditions and equipment parameters as set by the vendor. The usable range and optimum values of system parameters were determined. The testing simulated normal and adverse signal conditions to characterize the DABS processor. This phase also determined the performance of the lead edge and trail edge declaration logic, preamble detection logic, message bit processing logic, and the confidence bit assignment logic.

TEST PROCEDURES AND RESULTS—PHASE I

DABS MULTICHANNEL RECEIVER.

The following paragraphs describe the test procedures employed and the results obtained to determine the performance of the multichannel receiver.

LOG LINEARITY—SUM (Σ), DIFFERENCE (Δ), AND OMNI (Ω).

The main purpose of these tests was to verify that the log Σ, Δ, and Ω channels were linear over the dynamic range and frequency range of the receiver, and that the differential amplitudes were within the ±1.5 decibel (dB) specified in the ER requirements.

The basic system for data açquistion is shown in figure 1. Measurements were made for RF input continuous wave (CW) levels from -20 decibels above 1 milliwatt (dBm) to -88 dBm at 1090 megahertz (MHz) and from 1087 to 1093 MHz in 1 MHz increments. The output of the log amplifiers was connected to a digital voltmeter for relative amplitude measurements ranging over the dynamic and frequency ranges for Σ, Δ, and Ω.

Figures 2, 3, and 4 depict the linear and transfer characteristics for CW inputs of equal amplitudes over the dynamic and frequency ranges for Σ, Δ, and Ω. Analysis of the plots indicate that each channel tracked linearly within ±1.5 dB. The test verified the bandwidth frequency response to be flat to within ±0.1 dB from 1087 to 1093 MHz.

DIFFERENCE/SUM (Δ/Σ) CURVE MEASUREMENTS.

The purpose of this test was to verify the monopulse range and operating frequency range of the receiver. In addition, the Δ/Σ peak-to-peak variation was measured to verify the FAA-ER-240-26 requirement that this variation did not exceed $0.10\ (1+\left|\frac{\Delta}{\Sigma}\right|^2)$ for Δ/Σ within the calibration limits.

The general test configuration used to collect data is shown in figure 1. The Σ and Δ outputs of the RFTU were adjusted with a vector voltmeter to Σ = -50 dBm and Δ = -50 dBm at a

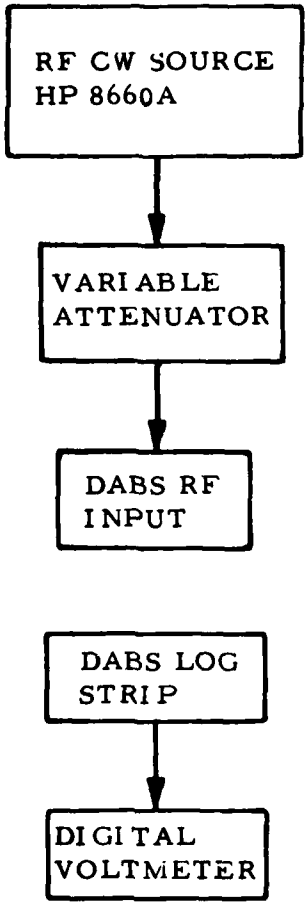

TEST POINTS
LOG Σ 1A3A8 - PIN 1
LOG Δ 1A3A8 - PIN 5
LOG Ω 1A3A8 - PIN 3

80-11-1

FIGURE 1. LOG LINEARITY TEST CONFIGURATION

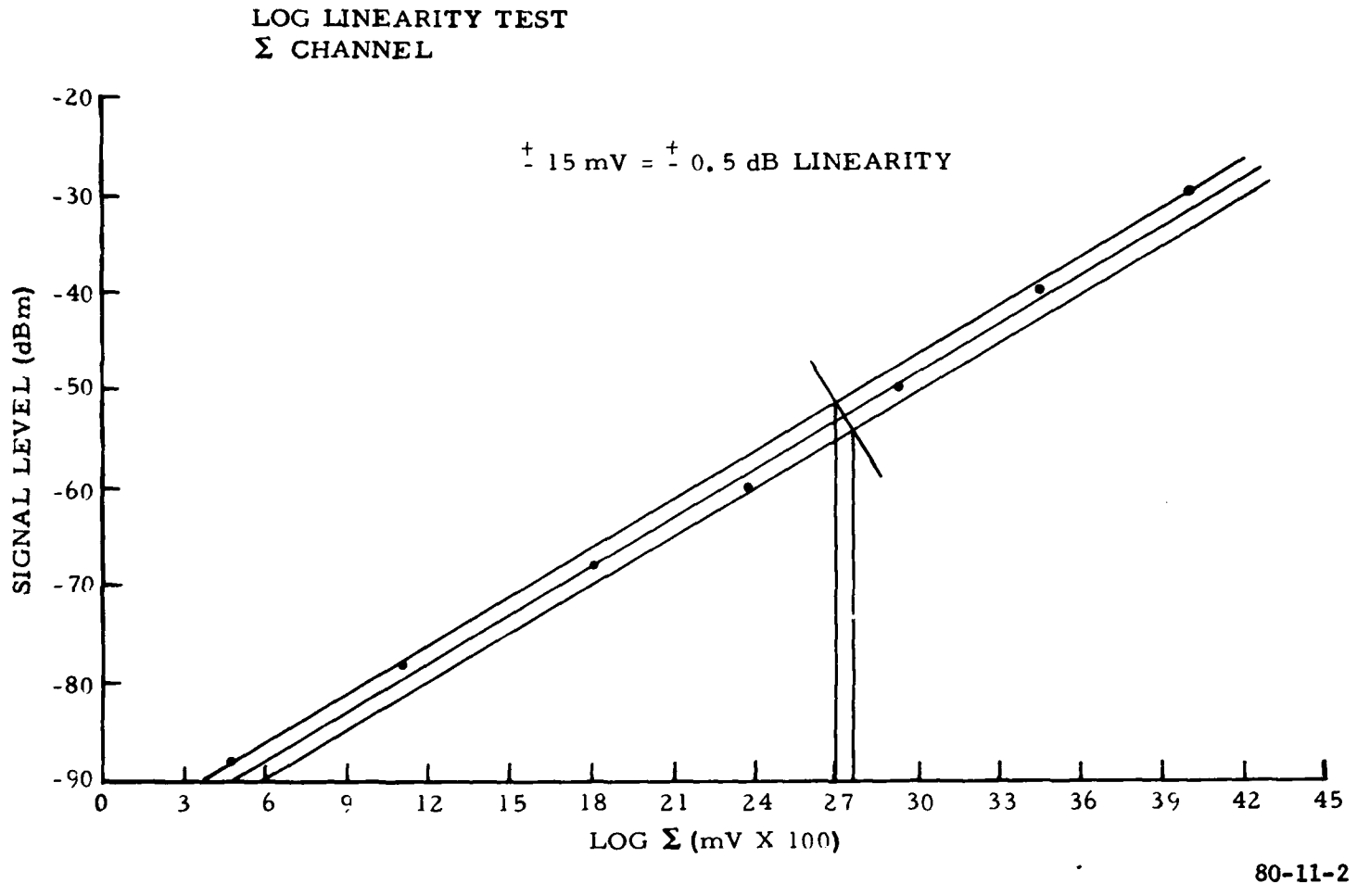

FIGURE 2. LOG Σ LINEARITY

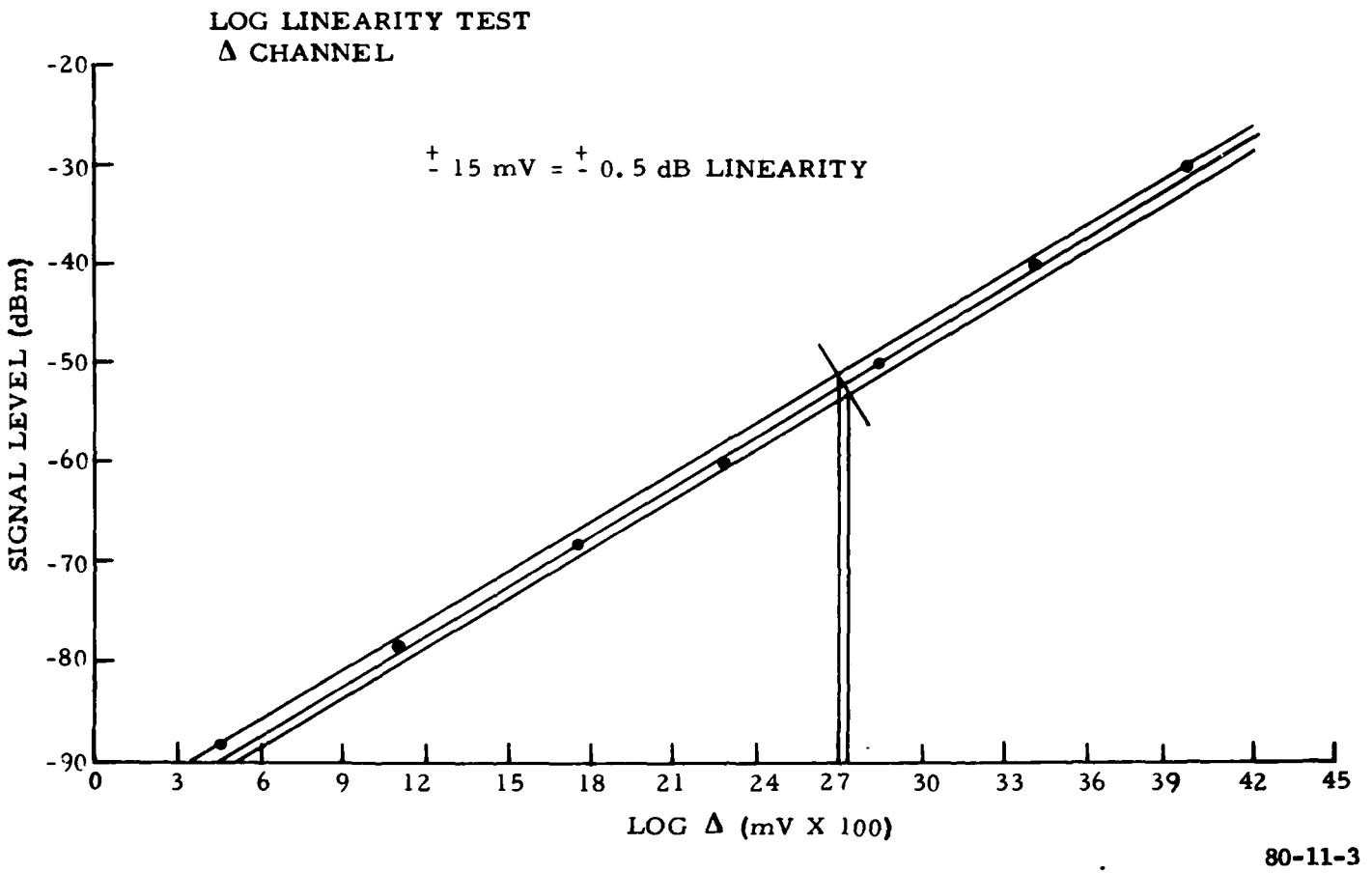

FIGURE 3. LOG Δ LINEARITY

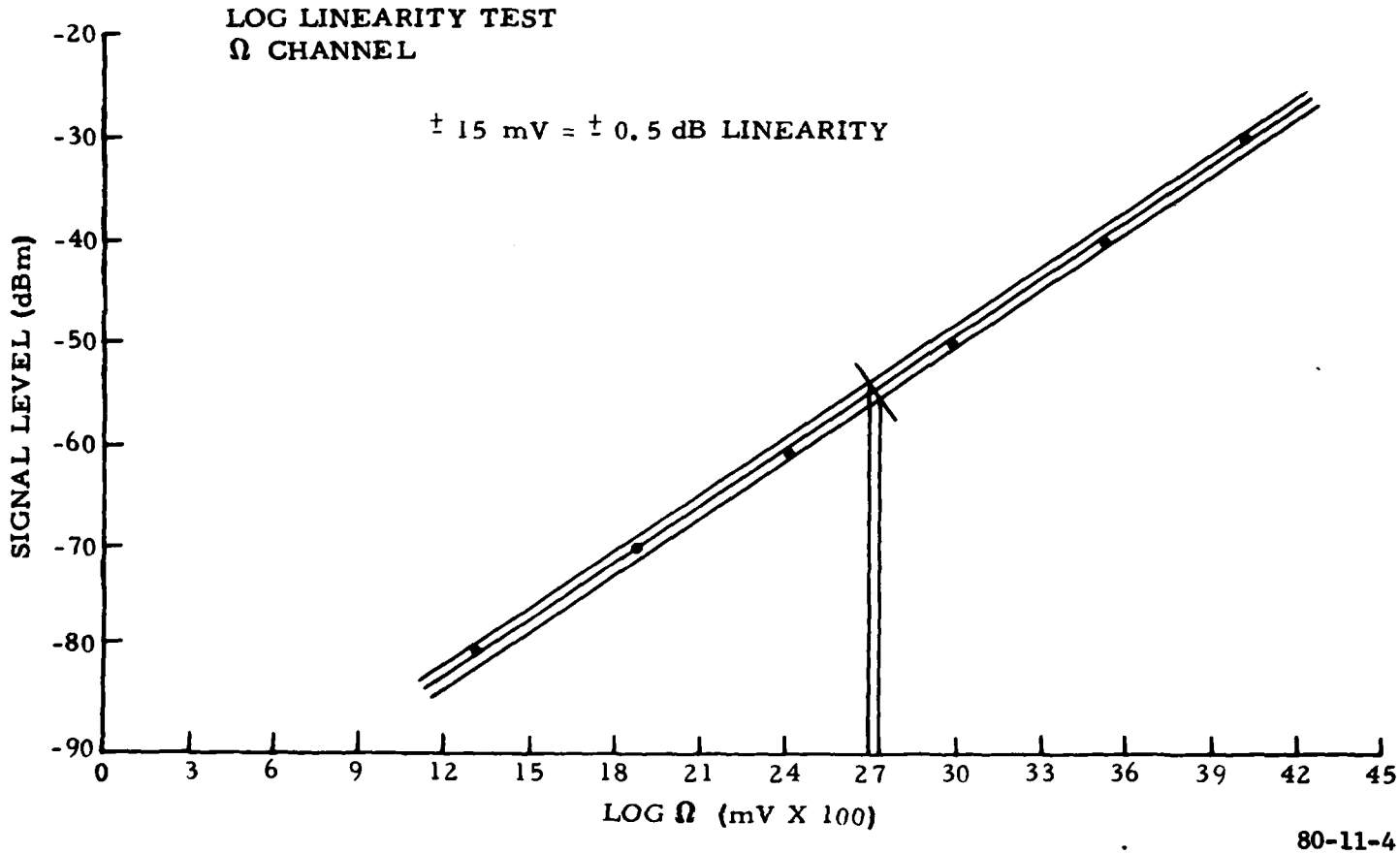

FIGURE 4. LOG Ω LINEARITY

frequency of 1090 MHz. These values, defined in FAA-ER-240-26, generate monopulse calibration curves. A calibration curve was derived for the monopulse channel to define the relationship between the ratio Δ/Σ at the input to the receiver and the monopulse video output. The calibration curve was obtained by varying the Δ amplitude signal level between 0 and -37 dBm. A digital voltmeter measured the receiver phase delay board output, which varied between 0 and -2.55 volts. Figure 5 is a plot of the monopulse calibration curve.

Monopulse accuracy data were collected for an input signal level of -50 dBm over the frequency range of 1090 ±3 MHz. The monopulse calibration curve was used to convert the output variation values in millivolts (mV) to Δ/Σ input ratio values. Figure 6 depicts monopulse channel accuracy. The upper curve is a tolerance plot of 0.1 $(1+ |\frac{\Delta}{\Sigma}|^2)$ for Δ/Σ ratios between -1.25 and +1.25. The scatter plot just below the tolerance curve presents the total variation in Δ/Σ ratio for each condition tested. For each value of Δ/Σ, maximum and minimum mV values were converted to Δ/Σ ratios from the monopulse calibration curve. After the Δ/Σ ratios were defined, their total variation was calculated and plotted. The scatter plot shown in figure 6 verified the FAA-ER-240-26 requirement that the Δ/Σ peak-to-peak variation did not exceed 0.10 $(1+ |\frac{\Delta}{\Sigma}|^2)$ for Δ/Σ within the calibration limits. In addition, the maximum variation from the calibration curve did not exceed 0.074 $(1+ |\frac{\Delta}{\Sigma}|^2)$.

VIDEO DIGITIZER.

The analog inputs to the video digitizer from the log amplifiers are: the log $|\Sigma|$, the log $|\Delta|$, and the log $|\Omega|$. The video digitizer generates seven outputs:

1. QΣPS, Quantized sum positive slope

2. QΣNS, Quantized sum negative slope

3. QΣD, Quantized sum DABS

4. QΣA, Quantized sum ATCRBS

5. QSLSD, Quantized side lobe suppression DABS

6. QSLSA, Quantized side lobe suppression ATCRBS

7. CAC, Chip amplitude compare

QΣPS and QΣNS indicate the width of a log $|\Sigma|$ pulse by accurately defining the location of the leading and trailing edges. QΣD and QΣA indicate whether the log $|\Sigma|$ exceeds threshold sum DABS ($T_{\Sigma D}$) or composite threshold ATCRBS ($T_{\Sigma A}$). This composite threshold was equal to the instantaneous amplitude of either the fixed threshold, adaptive threshold, or the sensitivity time control threshold, whichever was the most positive. QSLSD and QSLSA determine whether the source of the received reply signal is within a designated sector of the sensor's antenna main beam. CAC was employed to establish a proper timing relationship of system signals and aids in determining the validity and confidence levels of data bits.

VIDEO QUANTIZER PULSE DETECTION.

The purposes of the pulse detection tests were to: (1) statistically determine the operating range of the receiver video quantizer; (2) determine the effects the adjustable parameters threshold positive slope (T_{PS}), threshold negative slope (T_{NS}), $T_{\Sigma A}$, and $T_{\Sigma D}$ had on the sensitivity of the video pulse quantizer (VPQ) pulse detection ability; and (3) determine the optimum adjustments of the above parameters.

The basic test configuration for data acquisition is shown in figure 7. Measurements were made over the frequency range of 1090 ±3 MHz and amplitude range of -20 dBm down to -79 dBm for a standard RF test pulse as defined in the FAA-ER-240-26. Each of the

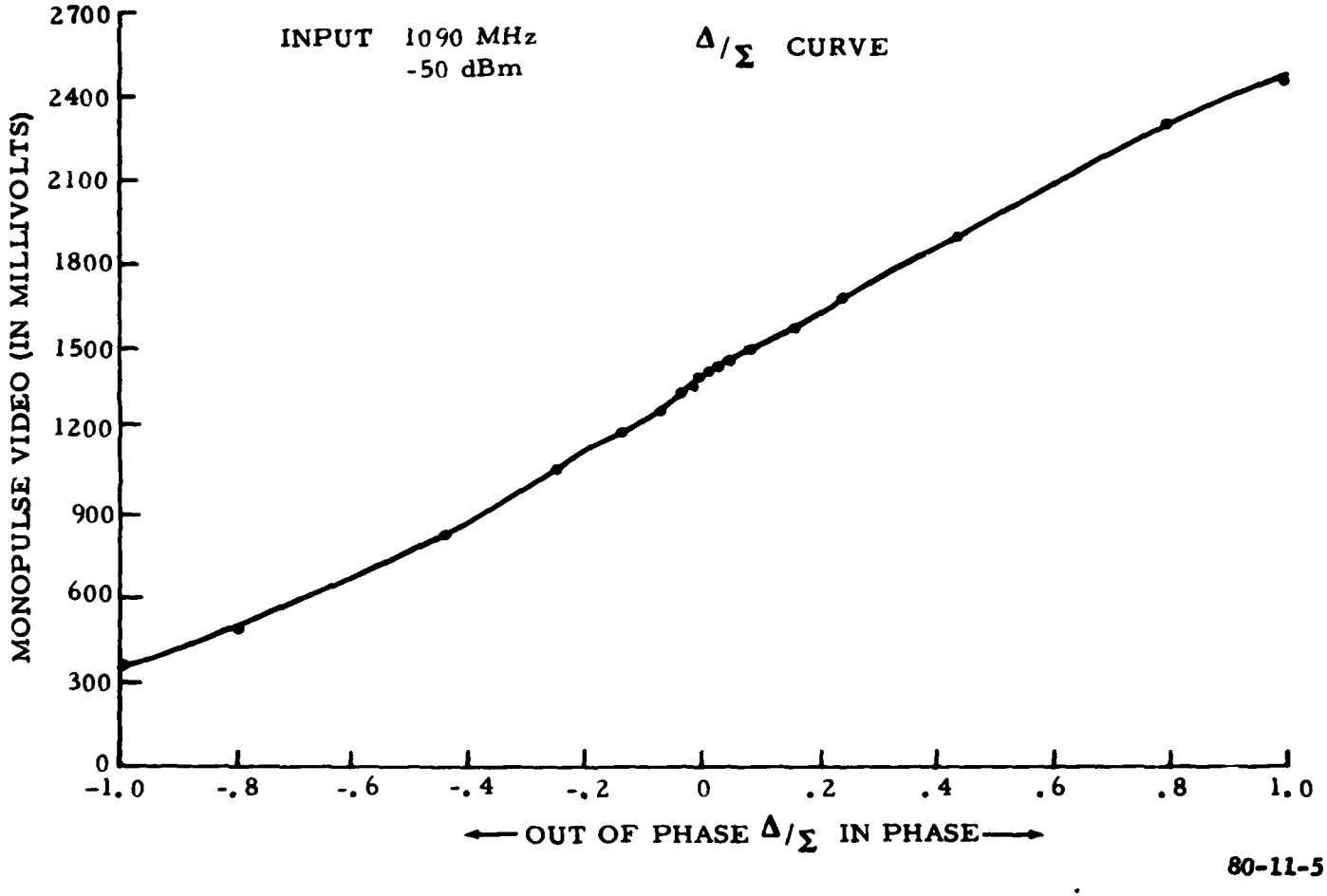

FIGURE 5. MONOPULSE CALIBRATION CURVE

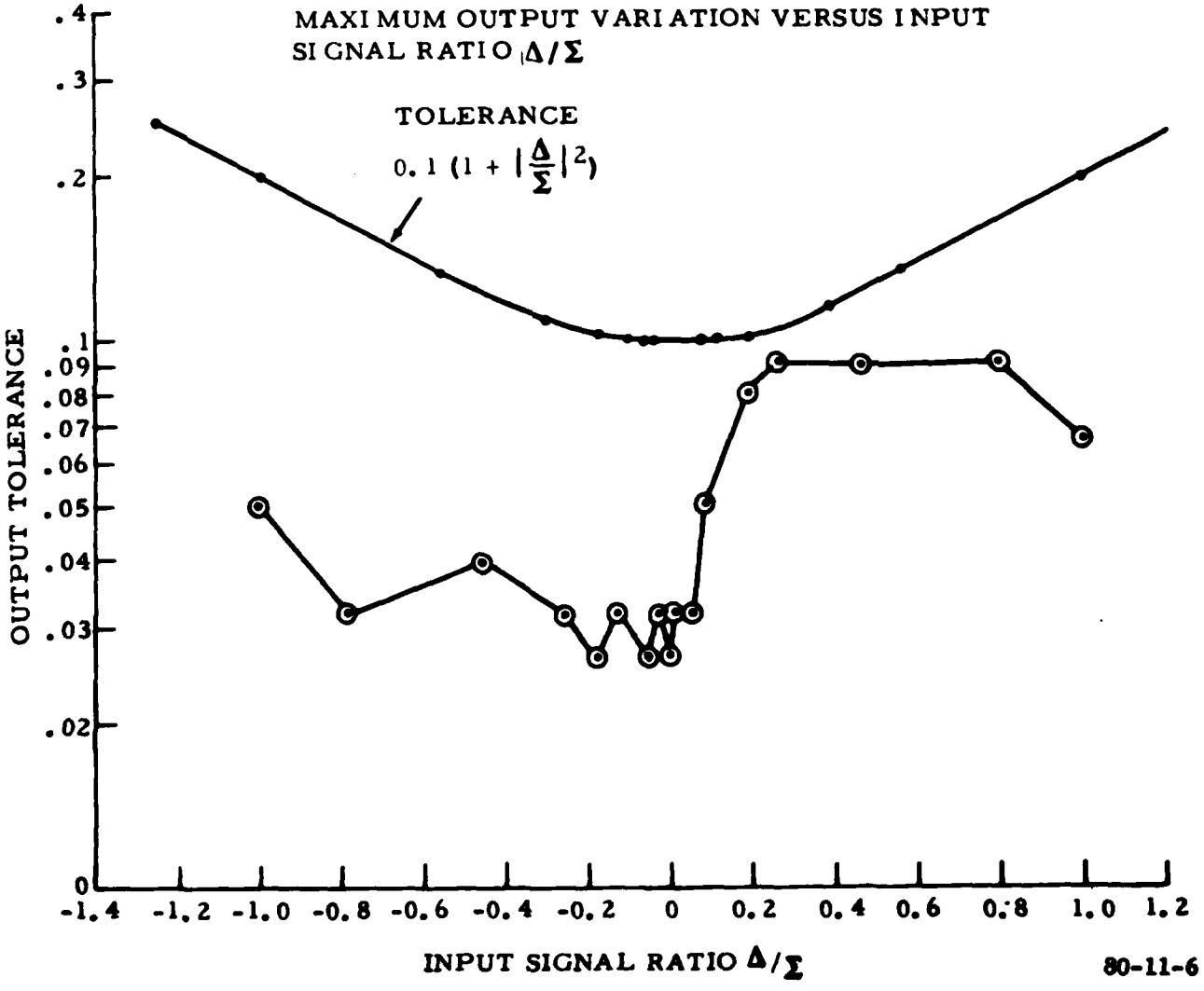

FIGURE 6. DABS MONOPULSE CHANNEL ACCURACY

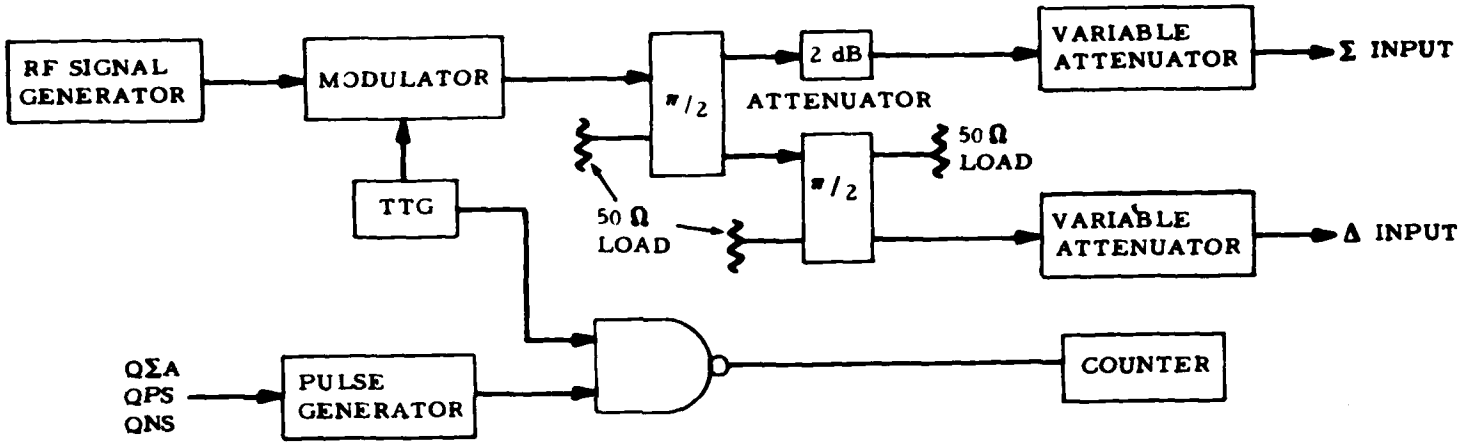

T_{NS} = + 148 mV

T_{PS} = - 149 mV

T_{Ω} = + 750 mV

T_{Δ} = - 300 mV

$T_{\Sigma D}$ = + 669 mV

T_{FD} = + 625 mV

$T_{\Sigma A}$ = + 623 mV

T_{FA} = + 618 mV

80-11-7

FIGURE 7. VPQ TEST CONFIGURATION

adjustable threshold parameters was varied independently over its operating range and the quantized counts recorded.

Analysis of the results indicated that for the threshold values in figure 7 an RF signal input at the sensor RF port of -79.0 dBm or greater would be detected with a 90 percent reply probability in the absence of all environmental fruit and synchronous garble.

QUANTIZED SIDE-LOBE SUPPRESSION ATCRBS (QSLSA) AND QUANTIZED SIDE-LOBE SUPPRESSION DABS (QSLSD).

These tests were performed to determine the effects the difference and omni-adjustable threshold parameters had on receiver performance over a range of main beam/side-lobe ratios. Only those replies with azimuth between the angles of positive and negative crossover were declared valid. This was accomplished by comparing the amplitude of log $|\Sigma|$, log $|\Delta|$, and log $|\Omega|$. Two conditions must be met: (1) (log $|\Sigma|$ - log $|\Omega|$) > omnithreshold and (log $|\Sigma|$ - log $|\Delta|$) > difference threshold, and (2) log $|\Sigma| > T_{\Sigma}$. Figure 8 is a simplified schematic diagram showing the generation of QSLSA and QSLSD output signals.

The first test collected data on the performance of the difference threshold and QSLSD on the QSLSA outputs. Evaluation of the difference threshold effects was accomplished by terminating the log $|\Omega|$ input and adjusting the omni-threshold voltage to -700 mV. This procedure satisfied the condition of (log $|\Sigma|$ - log $|\Omega|$) > T_{Ω}. Three main beam/side-lobe ratios were tested at three signal amplitudes (-20 dBm, -50 dBm, and -79 dBm). The ratios were as follows: (1) $\Delta = \Sigma$ +3 dB, a signal outside the main beam crossover point; (2) $\Delta = \Sigma$, a signal on the crossover point; and (3) $\Delta = \Sigma$ -3dB, a signal in the main beam between the crossover points. The second test collected similar data for various omnithreshold values and difference threshold = -700 mV.

The results for variations of omni-threshold were used to determine the effect it had on received signals. An adjustment of the omnithreshold aided in determining whether the source of the received signal was within a designated sector of the antenna beam width. Final adjustment of the omnithreshold will be determined by factors such as the main beam side-lobe amplitude and the amplitude of the omniantenna pattern. Analysis of the antenna patterns available for both the main beam and omniantennas suggest a reasonable value for the omnithreshold would be +750 mV ($\approx$13 dB).

ADAPTIVE THRESHOLD (TADAP).

The purpose of this test was to determine if any loss of valid target replies occurred when the maximum adaptive threshold parameter value was used to reduce low level multipath signals. This test also varied the time interval (T) that the adaptive threshold remained in operation after a reply pulse was received to determine if any loss of valid replies occurred.

The QΣD and QΣA signals indicate whether the log $|\Sigma|$ received signal exceeded an adjustable composite threshold. The composite threshold was equal to the instantaneous amplitude of a fixed threshold, adaptive threshold, or a sensitivity time control threshold, whichever was the most positive.

Incoming log $|\Sigma|$ video pulses were sampled by the adaptive threshold circuit. This circuit provided a constant threshold value below peak amplitude for the sampled pulse. For each video pulse exceeding the composite threshold, the adaptive threshold was automatically reset to a value below the peak of the sampled pulse. The difference between the peak of the sampled video pulse and the adaptive threshold level set, K, was site adjustable. The value K blanked low-level multipath reply pulses.

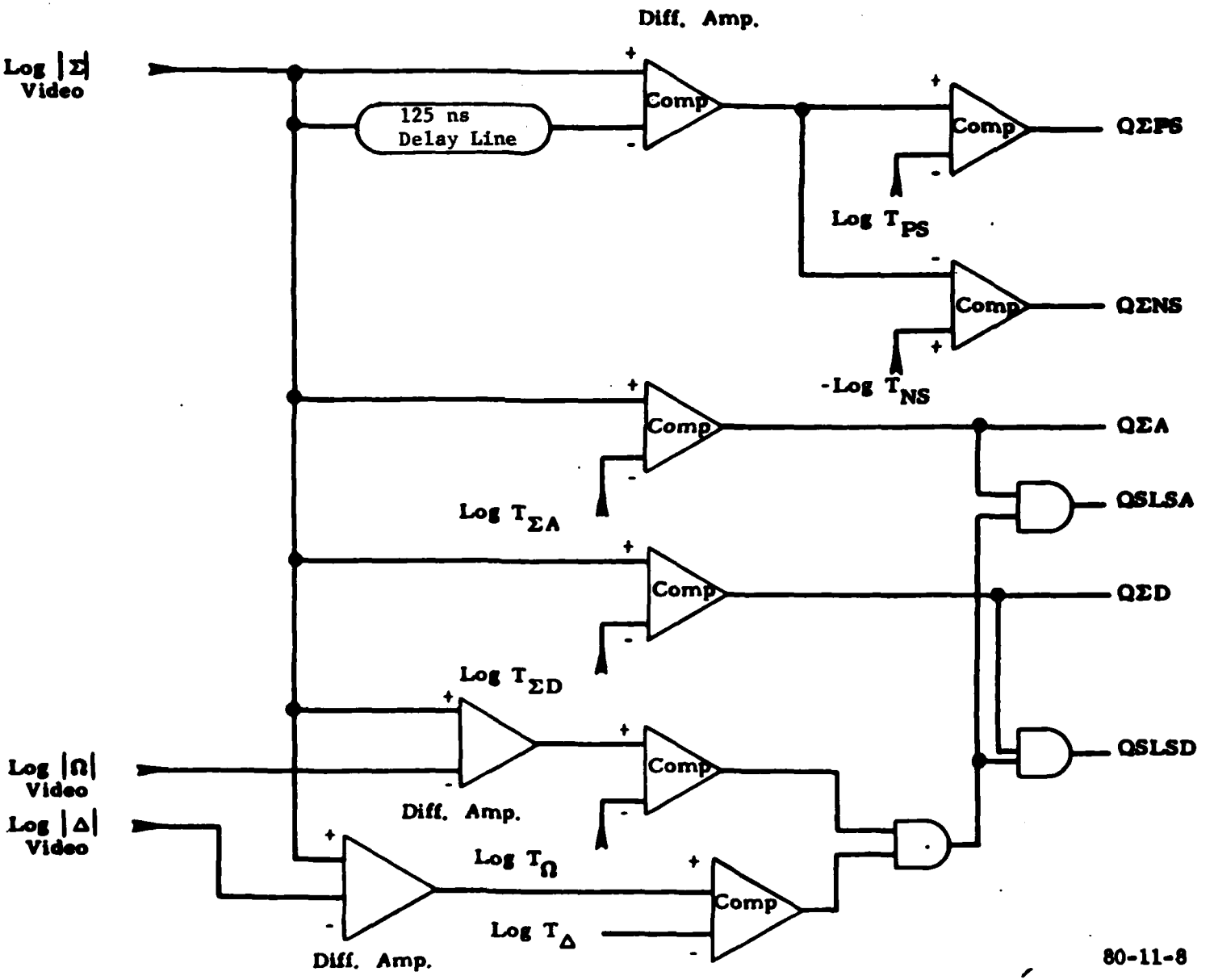

FIGURE 8. QSLSD AND QSLSA SIGNAL GENERATION SIMPLIFIED SCHEMATIC DIAGRAM

A general functional diagram of the test configuration is shown in figure 9. Two pulse generators simulated the log $|\Sigma|$ video pulses of a reply. The spacing between these pulses was adjusted by the switch delays of the TTG. Each pulse was used to modulate a 1090 MHz CW source and varied independently in amplitude. Adaptive threshold values were tested for: K=25 dB and T=20 microseconds (μs), K=15 dB and T=20 μs, and K=15 with T=1.0 μs.

The results of these tests, figures 10, 11, and 12, indicate no loss of valid target replies. For each video pulse that exceeded the composite threshold, the adaptive threshold was set to the correct value below the reply pulse amplitude. Simulated low level multipath reply signals were suppressed when the adaptive threshold was activated. Values of K=25 dB and T=10 μs were made as final adjustments for optimum target detection and multipath signal rejections.

TEST PROCEDURES AND RESULTS—PHASE II

ATCRBS REPLY PROCESSOR.

This section defines the tests and procedures used to identify the static performance of the ATCRBS reply processor subsystem. The function of the processor was to search the received pulse train for framing pulse pairs, and determine which ATCRBS code pulses were present for each reply. The purpose of these tests was to identify the characteristics of the subsystem and to optimize the variable parameters. The variable parameters identified the performance of each element in the subsystem.

The test performance of the lead and trail edge estimators, bracket detection, ATCRBS monopulse correlation, garble recognition, and confidence bit assignment is outlined below. In addition, tests were conducted to measure the influence of ATCRBS monopulse correlation parameter k on reply azimuth accuracy. Figure 13 is a block diagram of the ATCRBS reply processor.

LEAD AND TRAIL EDGE ESTIMATORS.

These tests measured the performance of the ATCRBS video digitizer's leading and trailing edge declaration logic and pseudo-leading edge generator. The FAA-ER-240-26 rules were complied with for the declaration of: leading edges (LE's), trailing edges (TE's), pseudo-leading edges, and narrow pulse rejection.

The ATCRBS VPQ contained a pseudo-leading edge generator which measured the width of each log video pulse. If the pulse width exceeded the threshold set to the nominal ATCRBS pulse width, one or more additional lead edges were generated. The additional lead edge pulses (pseudo-pulses) were obscured because of overlapping when inserted into the sum lead edge (ΣLE) serial data stream.

The tests were divided into two categories. The first was a series of static tests which generated pulses of K width, power, rise, and decay times.

Figure 14 is the basic test configuration for data acquisition. Initially, a standard test pulse having a width of 450 nanoseconds (ns), a 100-ns rise time, and a 150-ns decay time was inserted into the Σ input of the receiver at signal levels of -20 dBm, -50 dBm, and -79 dBm. For each of these pulse parameters, an analysis was performed to determine the correct occurrence of QΣA, quantized positive slope (QPS), quantized negative slope (QNS), and ΣLE pulse generation.

Results of the initial VPQ test indicated successful generation of ΣLE pulses in the serial output data stream.

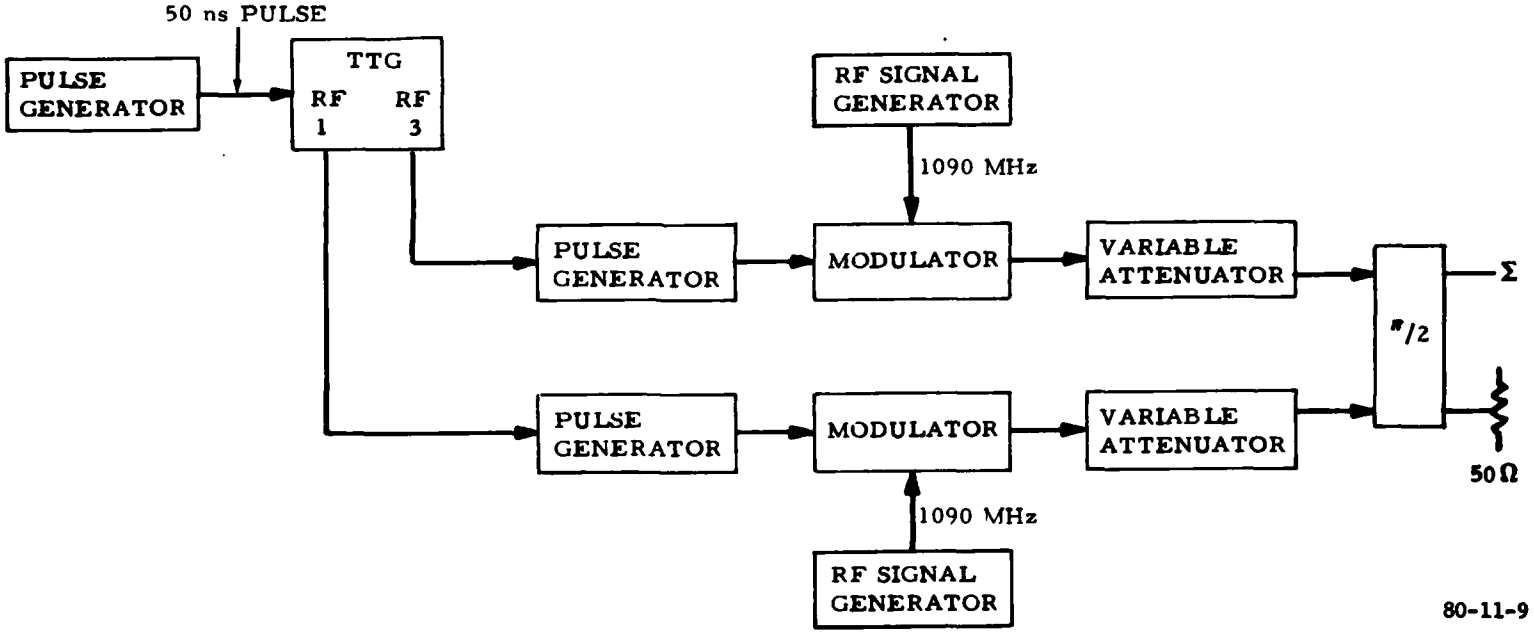

FIGURE 9. ADAPTIVE THRESHOLD TEST CONFIGURATION

ADAPTIVE THRESHOLD
K = 15 dBm T = 1.0 μs

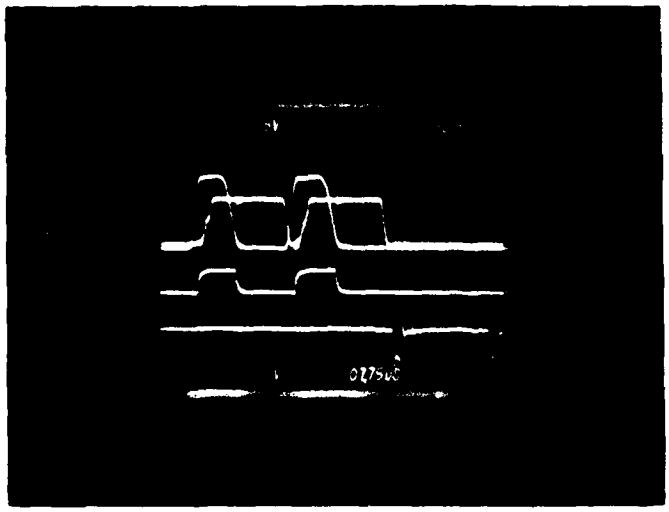

CHANNEL
1-LOG VIDEO
2-THRESHOLD ΣA
3-QΣA
4-SLE
INPUT 1
POWER -50 dBm
INPUT 2
POWER -50 dBm
SPACING 1.5 μs

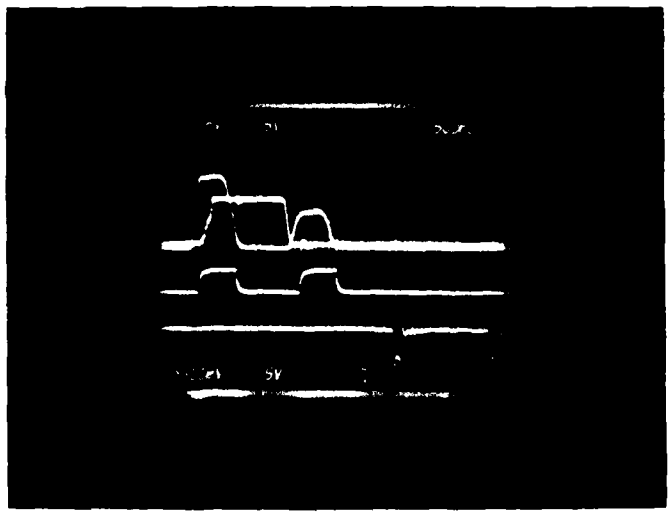

CHANNEL
1-LOG VIDEO
2-THRESHOLD ΣA
3-QΣA
4-SLE
INPUT 1
POWER -50 dBm
INPUT 2
POWER -70 dBm
SPACING 1.5 μs

80-11-10

FIGURE 10. ADAPTIVE THRESHOLD K=15 dB AND T=1.0 μs

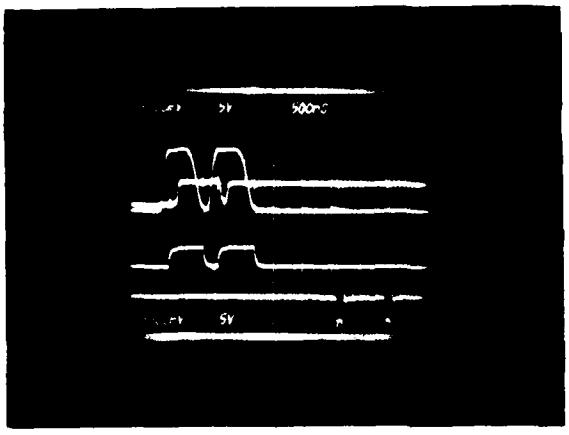

ADAPTIVE THRESHOLD
K = 25 dB T = 20 μs

CHANNEL
1-LOG VIDEO
2-THRESHOLD ΣA
3-QΣA
4-SLE
INPUT 1
POWER -50 dBm
INPUT 2
POWER -50 dBm
SPACING 800 ns

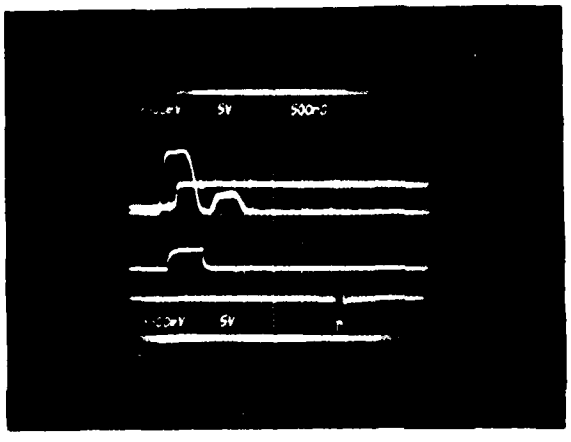

CHANNEL
1-LOG VIDEO
2-THRESHOLD ΣA
3-QΣA
4-SLE
INPUT 1
POWER -50 dBm
INPUT 2
POWER -80 dBm
SPACING 800 ns

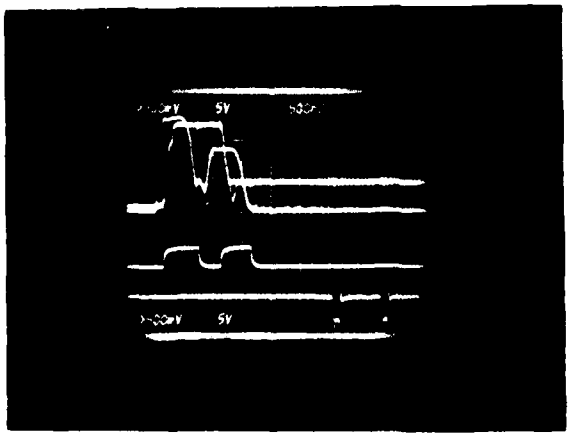

CHANNEL
1-LOG VIDEO
2-THRESHOLD ΣA
3- QΣA
4-SLE
INPUT 1
POWER -20 dBm
INPUT 2
POWER -50 dBm
SPACING 800 ns

80-11-11

FIGURE 11. ADAPTIVE THRESHOLD K=25 dB AND T=20 μs

ADAPTIVE THRESHOLD
K = 15 dBm T=20 μs

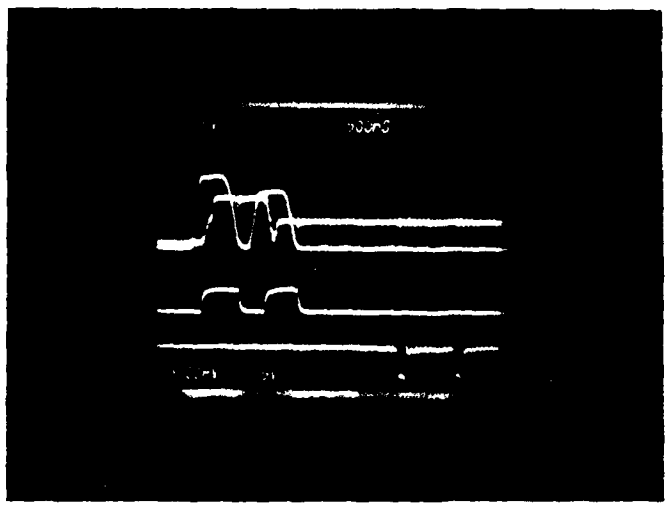

CHANNEL
1-LOG VIDEO
2-THRESHOLD Σ A
3-QΣA
4-SLE
INPUT 1
POWER -50 dBm
INPUT 2
POWER -60 dBm
SPACING 800 ns

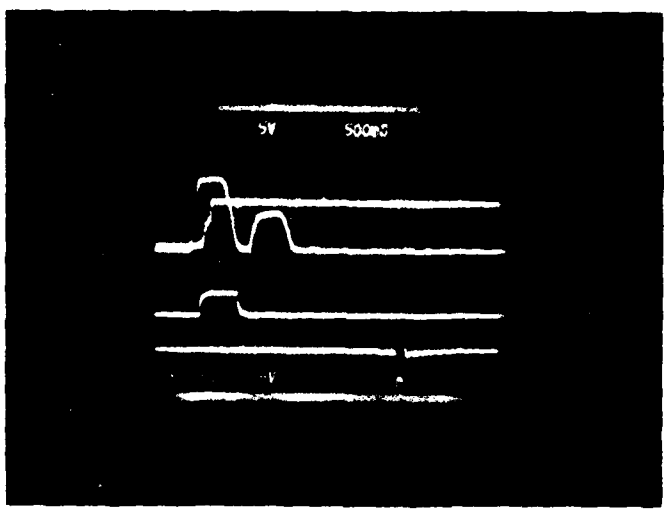

CHANNEL
1-LOG VIDEO
2-THRESHOLD Σ A
3-QΣA
4-SLE
INPUT 1
POWER -50 dBm
INPUT 2
POWER -70 dBm
SPACING 80 ns

80-11-12

FIGURE 12. ADAPTIVE THRESHOLD K=15 dB AND T=20 μs

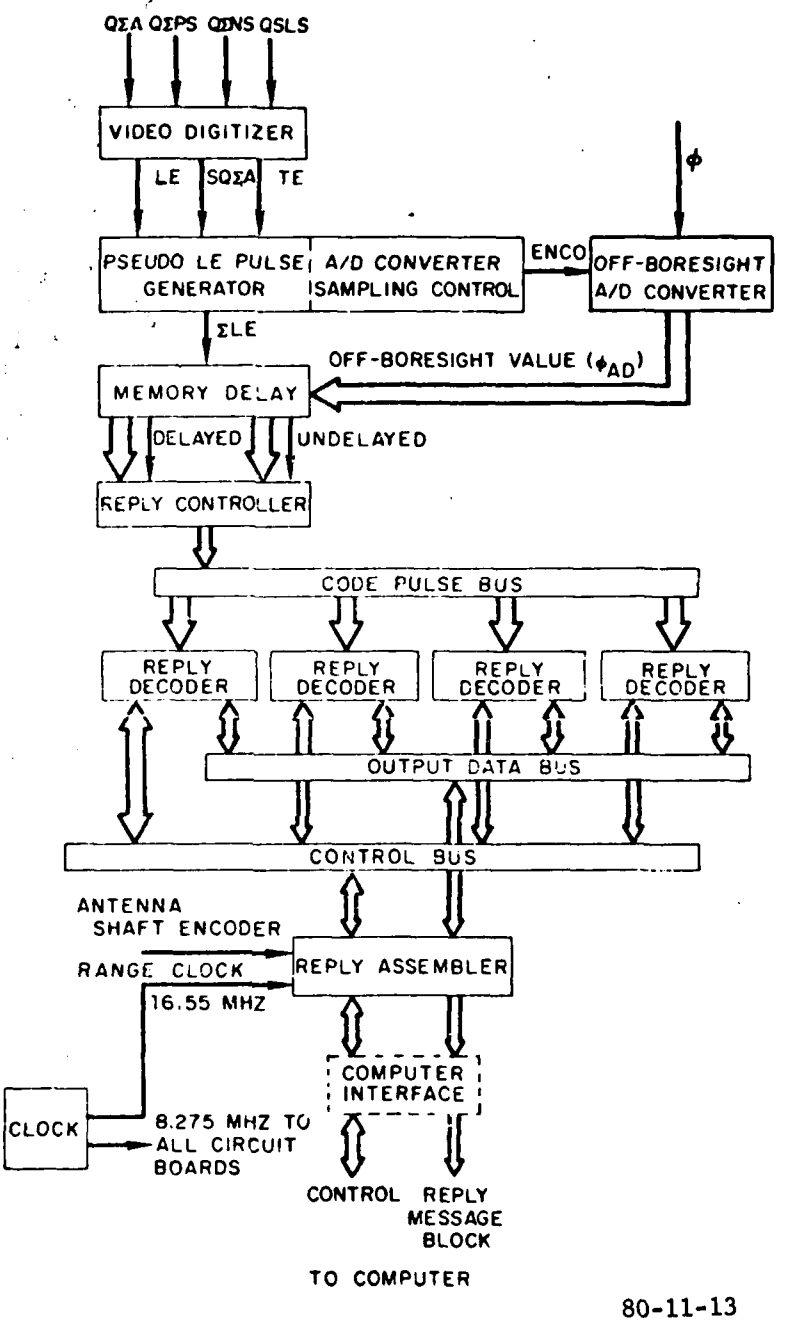

FIGURE 13. ATCRBS REPLY PROCESSOR, BLOCK DIAGRAM

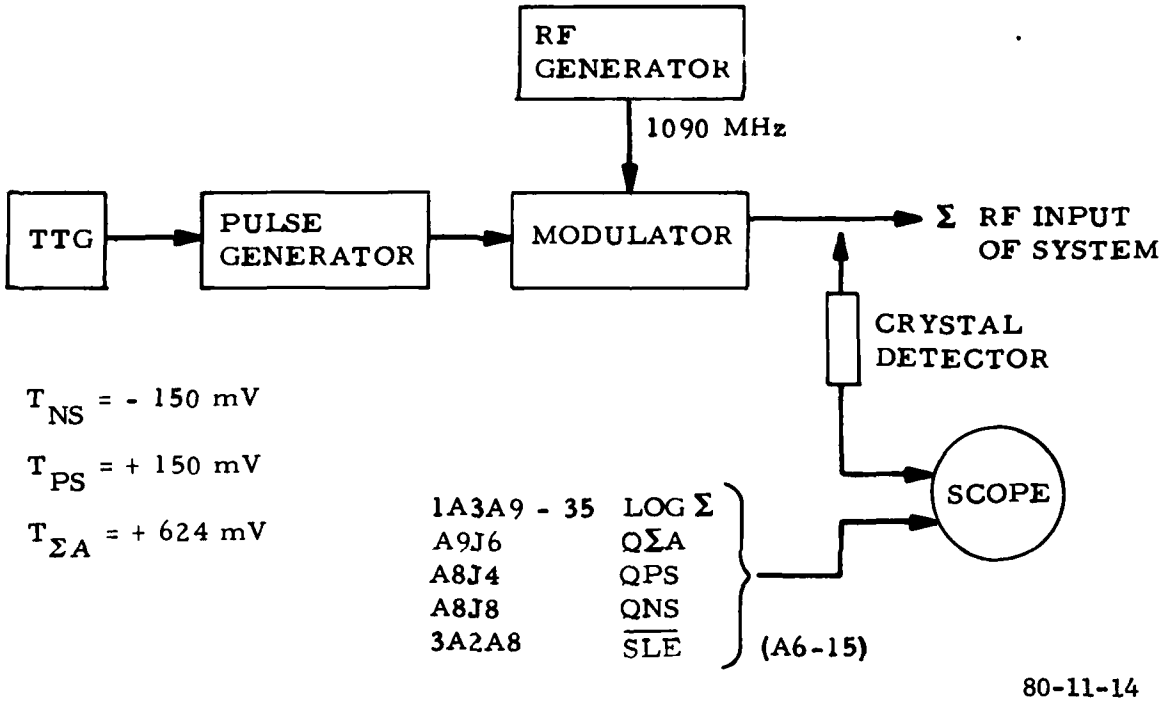

FIGURE 14. LEAD EDGE AND TRAIL EDGE DETECTION TEST CONFIGURATION

The next test determined the ATCRBS VPQ pseudo-leading edge generator performance. A test pulse was inserted into the Σ input port at -50 dBm with a standard rise time of 100 ns, decay time of 150 ns, and pulse widths of 600, 800, and 1,200 ns. Analysis of the ΣLE data stream indicated correct insertion of the pseudo-lead edges and compliance with the FAA-ER-240-26 values.

The second category of tests employed the test target generator. The test target generator was manually programmed to generate a pulse in RF channels 1 and 3 of reply data memory. Overlapping pulse conditions were simulated by offsetting one channel bias data group to the other. Figure 15 depicts the basic test configuration for input pulse widths of 200 ns and 350 ns.

Examination of the ΣLE data stream indicated correct narrow pulse rejection. In overlapping reply conditions, a wider QΣA resulted, pseudo-lead edges were generated, and the VPQ declared LE's for both of the pulses. When the amplitude of the second pulse had a QPS (t_1) = 1 and a QPS (t_1+d) = 0, the VPQ declared both pulses to have LE's. Time t_1 denoted when the VPQ circuit declared a pulse leading edge and d represents a delay of 125 ±10 ns.

BRACKET DETECTION.

An ATCRBS reply was declared whenever two pulses separated by 20.3 μs (framing pulses F_1 and F_2) were located in the input ΣLE. These tests measured bracket detection as a function of RF levels and framing pulse spacings. A reply was accepted as valid if at least one ungarbled framing pulse was received by the antenna's main beam, and the reply was not a phantom. A phantom bracket is defined as a declared bracket whose F_1 pulse is a valid code pulse or framing pulse of one reply, and whose F_2 pulse is a valid code or framing pulse of another reply.

The basic test configuration for data acquisition is shown in figure 16. The TTG was employed to simulate the bracket F_1 and F_2 pulses. The width of each pulse was programmed to be 450 ns. The output of the bracket detection logic (DCBKT) was counted by an electronic counter. Measurements were made for input RF signal levels of -20 dBm, -50 dBm, and -70 dBm and for framing pulse spacings ranging from 20.05 to 20.30 μs in 50-ns increments. A count representing 100 percent detection was established for a bracket pair spaced 20.3 μs with a strong reply (-20 dBm). This count was used to reference all other bracket detect counts. The tests results are depicted in figures 17 and 18. Bracket detection was generated symmetrically around the nominal pulse position with 100 percent detection achieved within ±120.8 ns for signal levels of -70 dBm and above.

Measurements were made to determine the 90 percent bracket detection sensitivity. This was accomplished by attenuating the simulated test target generated bracket reply until the electronic counter displayed 90 percent of the established 100 percent reference count. It was determined that an RF test bracket reply of -79.0 dBm at the sensor RF input port provided 90 percent bracket detection capability in the absence of all environmental fruit.

Additional bracket detection tests were conducted as functions of simulated fruit environments. Bracket detection was near 100 percent for fruit levels up to and including 32,000 replies per second for strong (-50 dBm) bracket pairs and within ±100 ns of the 20.3 μs reference position. Detection was 98 percent for 32,000 fruit replies per second and -50 dBm signal level. A reduction in bracket detection resulted when the signal level was lowered to -70 dBm and mixed with ATCRBS fruit levels of 1,000 per second and above.

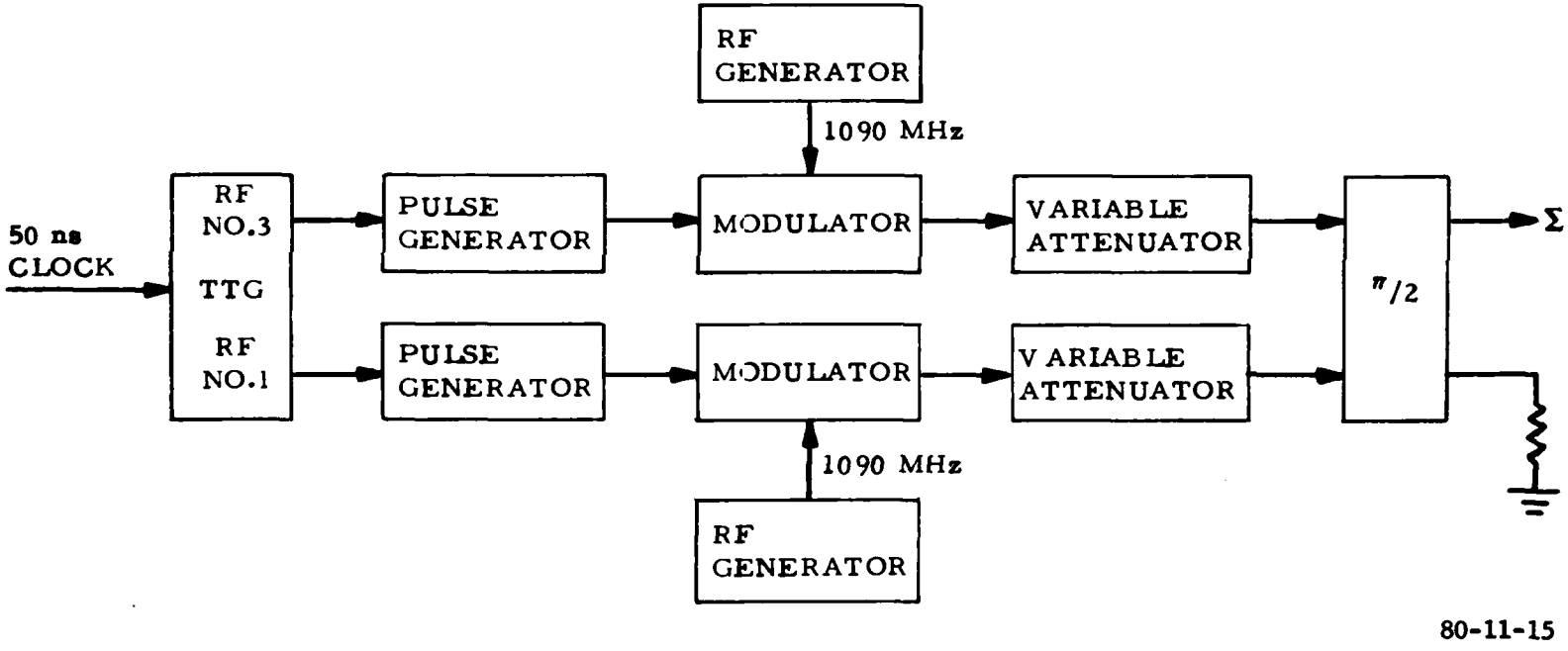

FIGURE 15. NARROW PULSE REJECTION AND WIDE PULSE DETECTION TEST CONFIGURATION

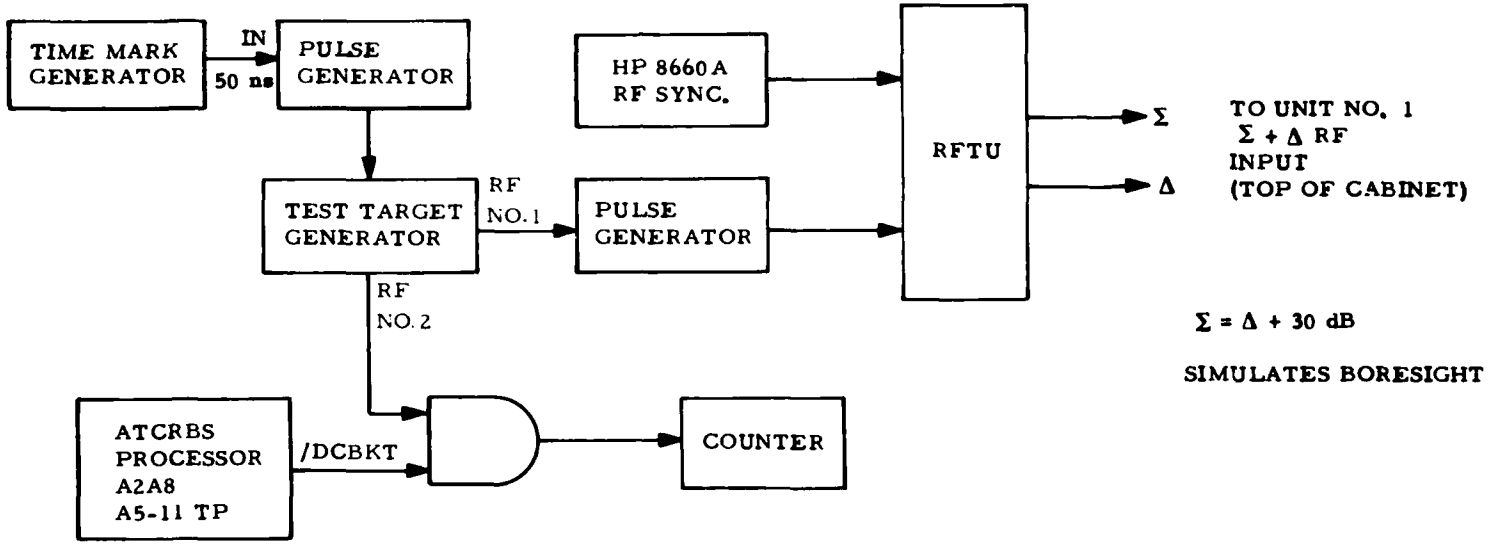

SYSTEM PARAMETERS

OMNI TERMINATED (50Ω)
ADAPTIVE THRESHOLD OFF
STC OFF
T_{Ω} = + 600 mV
T_{Δ} = + 000 mV

80-11-16

FIGURE 16. ATCRBS BRACKET DETECTION TEST CONFIGURATION

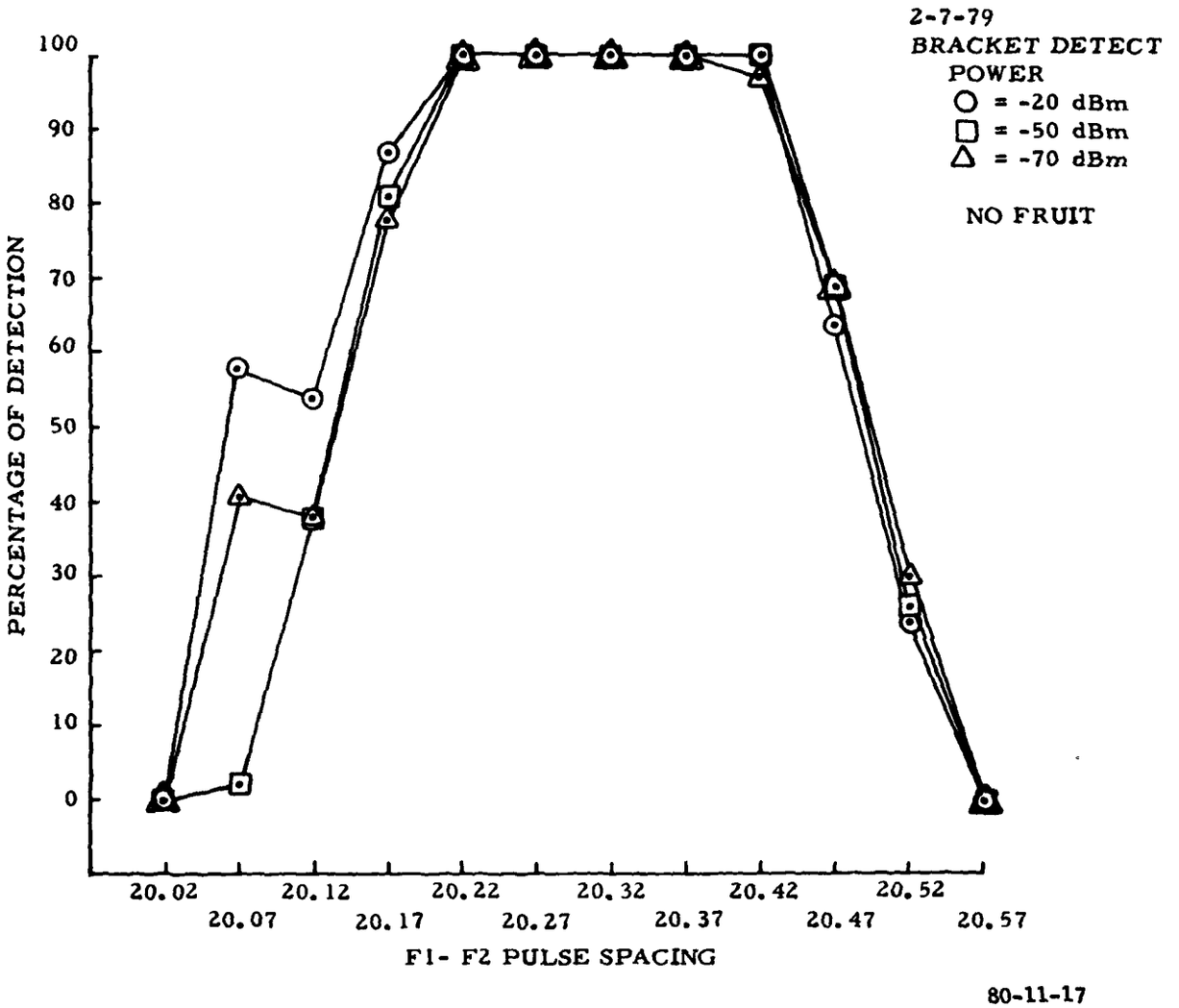

FIGURE 17. ATCRBS BRACKET DETECTION (ZERO FRUIT PER SECOND)

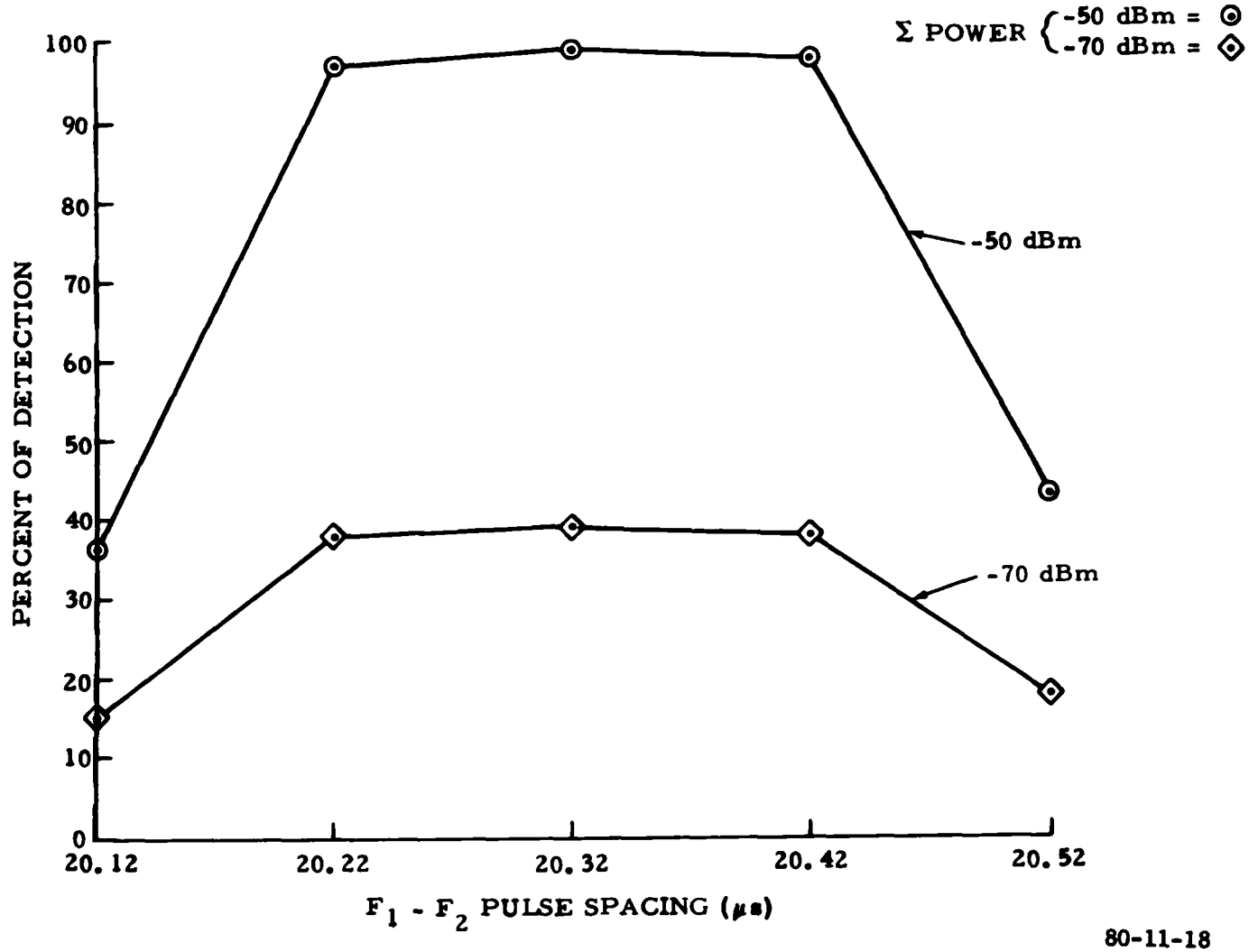

FIGURE 18. ATCRBS BRACKET DETECTION (32,000 FRUIT PER SECOND)

ATCRBS MONOPULSE CORRELATION CONSTANT—k.

These tests were designed to optimize the site-adjustable, monopulse correlation constant as a function of ATCRBS fruit levels. The ATCRBS monopulse correlation constant k was used to compare the monopulse sampled pulse value with the monopulse running average. A sample was correlated with the average providing that the sampled monopulse value differed from the average by a value less than or equal to k.

Configuration of the test system used for data acquisition is shown in figure 19. The tests were conducted for fruit rates of 0, 1, 2, 4, 8, 16, 20, and 32,000 replies per second using k values of 5, 8, 10, and 15. The test reply and fruit levels were applied to the DABS receiver. Reply information was recorded on magnetic tape via the DABS data extraction subsystem.

Recorded reply data were extracted by a PDP-11/45 computer program named "Garble Statistics Program." The volume of data obtained from this program was sufficient to define the effect of k values as a function of fruit levels in reply decoding. Analysis of the computer program output indicated optimal overall reply decoding performance occurred when k equaled 10.

GARBLE RECOGNITION AND CONFIDENCE BIT ASSIGNMENT.

This test was designed to determine the occurrence of garbled replies and the confidence bit status associated with each reply of two overlapped reply trains.

The test configuration is also shown in figure 19. Two test target generator replies, with discrete mode A codes of 3506 and 4271, were placed approximately 10 nautical miles (nmi) in range to the left and right of antenna boresight. The amplitude of the sum input was adjusted to -50 dBm; the difference input was set equal to -53 dBm. The test target generator was used to delay one test reply relative to the other by 25 μs. The F_1 to F_2 framing pulse lead edges were reduced by intervals of 120 ns until the two replies became completely overlapped. The DABS data extraction subsystem recorded on magnetic tape 10 antenna scans of reply data for each interval of delay.

The PDP-11 computer system provided statistical summaries defining reply codes and code confidence bit status. The status of the confidence bits relied on monopulse value and pulse position. The DABS switch adjustable, monopulse correlation parameter k was equal to 10.

Results from the PDP-11 reduction program indicated that the pulse processing rules were in agreement with the FAA-ER-240-26 requirements for both clear and overlapped pulse positions. Replies were declared garbled during bracket detection when their F_1 pulse lead edge sample occurred in any of the 14 pulse intervals of a previously declared bracket pair.

DIGITAL ATCRBS PROCESSOR TESTS.

The next set of tests was similar to those conducted to evaluate garble recognition for ATCRBS overlapped replies. Two major differences existed: (1) the monopulse reply code assignment value was varied to determine the effect on reply pulse detection and confidence, and (2) these tests eliminated the RF front end of the DABS by operating the test target generator in the all-digital mode. Prior to these tests the test target generator operated in the IF/RF mode to simulate target replies input to the DABS receiver.

Code recognition and confidence bit assignment tests were divided into two phases. The first generated a scenario

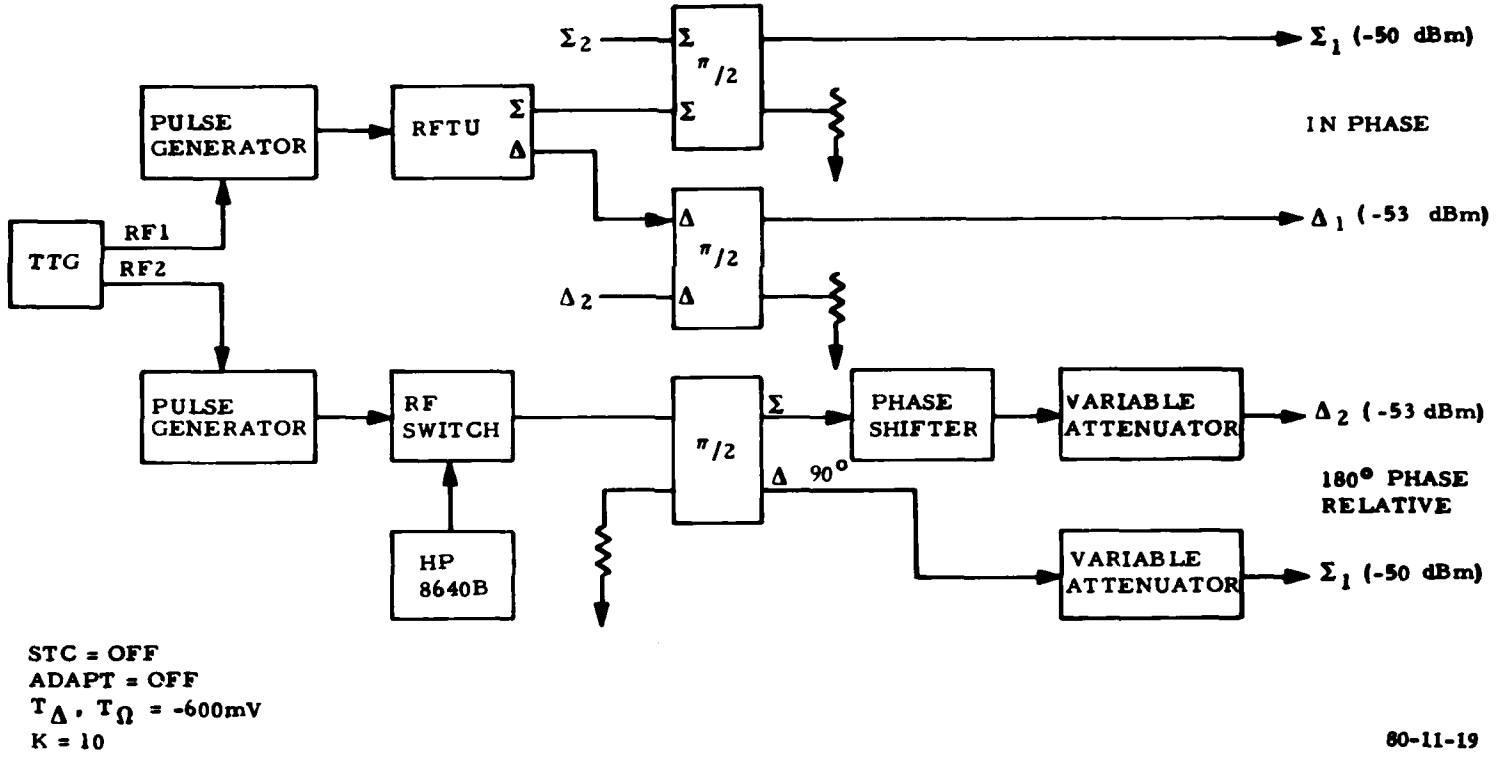

FIGURE 19. ATCRBS MONOPULSE CORRELATION TEST CONFIGURATION

for the test target generator to simulate two overlapping replies. The TTG scenario consisted of five pairs of overlapped replies with monopulse differences of 40, 20, 15, 10, and 5 (figures 20 and 21). The monopulse correlation parameter k was kept at 10 for these tests.

Following bracket detection, code pulses were associated with the reply on: (1) lead edge location, (2) monopulse sampled value, (3) monopulse arithmetic difference k, and (4) current monopulse average.

Analysis of the PDP-11 output listings of overlapped replies indicated a pattern. This occurred when two code trains were separated and the F_1 framing pulse of the second code train was coincident with the unused A_4 code pulse position of the first code train. The first reply code of 3506 was consistently decoded incorrectly as a 7506 reply code for monopulse differences of 40, 20, and 15; all of which were greater than the k value of 10. An incorrect A_4 code pulse resulted for the first reply correlated and was decoded with low confidence. These decoding errors resulted from a subtle flaw in the DABS engineering model specification which occurs when the leading bracket pulse of a later reply overlaps an A, B, C, or D code pulse of a previous reply. As a result of this test effort, the error has been corrected in the DABS Technical Data Package.

Additional analysis was made for overlapped replies with monopulse values equal to or less than k=10. Figure 22 illustrates this example. The results shown in figure 23 indicate more erroneous code pulse declarations and, in agreement with the code confidence decision rules (FAA-ER-240-26) for overlapped replies, more low confidence declarations.

The second phase of tests used a test target generator scenario to generate two replies that were overlapped and interleaved with two additional overlapped replies. Figure 24 depicts test reply positions.

Figure 25 depicts analysis of the PDP-11 computer listings indicating the undesirable situations at the reply decode level. In figure 25, one of the four test reply code trains (5221) failed to be declared. This was attributed to decoder capacity being reached before all valid replies had been processed. This occurred when many phantom replies resulted from overlapping and interleaving code trains. Bracket detection was prevented from entering a decoder and the reply was lost, but not before being detected by the overflow bit.

As before, when the code trains were separated and the F_1 framing pulse of the second code train was coincident with the unused A_4 code pulse position of the first code train, the A_4 pulse was inserted.

As indicated in the figure, the first reply (3506) was incorrectly decoded when the D_2 and B_4 pulses were not detected. This was caused by the operational design of the TTG and not the reply decoders. The TTG monopulse technique logically OR'ed the D_2 and B_4 monopulse values with the C_4 and A_4 monopulse values of the 4271 reply code train. The resulting test target generator monopulse value, generated for both reply code train pulses became 125. This prevented the D_2 and B_4 pulses from correlating with their reply.

REPLY MONOPULSE AVERAGE ESTIMATE.

This test measured the effect of varying the ATCRBS monopulse correlation parameter k on reply monopulse average estimates as a function of off-boresight angle. The DABS data extraction subsystem was used to collect reply data from the DABS calibration performance monitoring equipment (CPME). The CPME provided ATCRBS replies at a known fixed

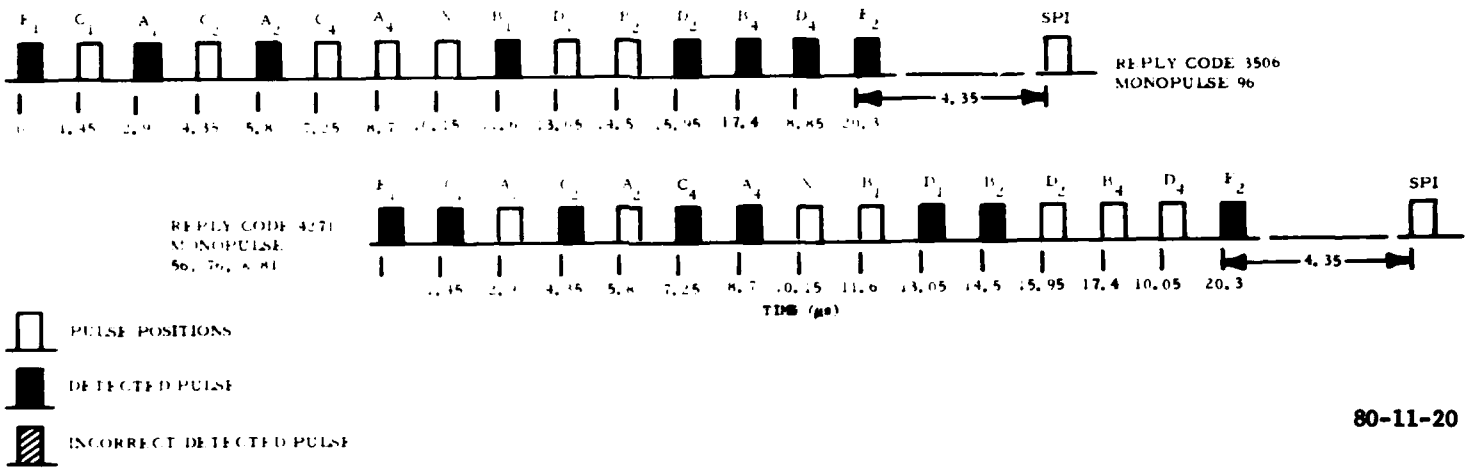

FIGURE 20. TEST GENERATED REPLIES MONOPULSE DIFFERENCES OF 40, 20, AND 15

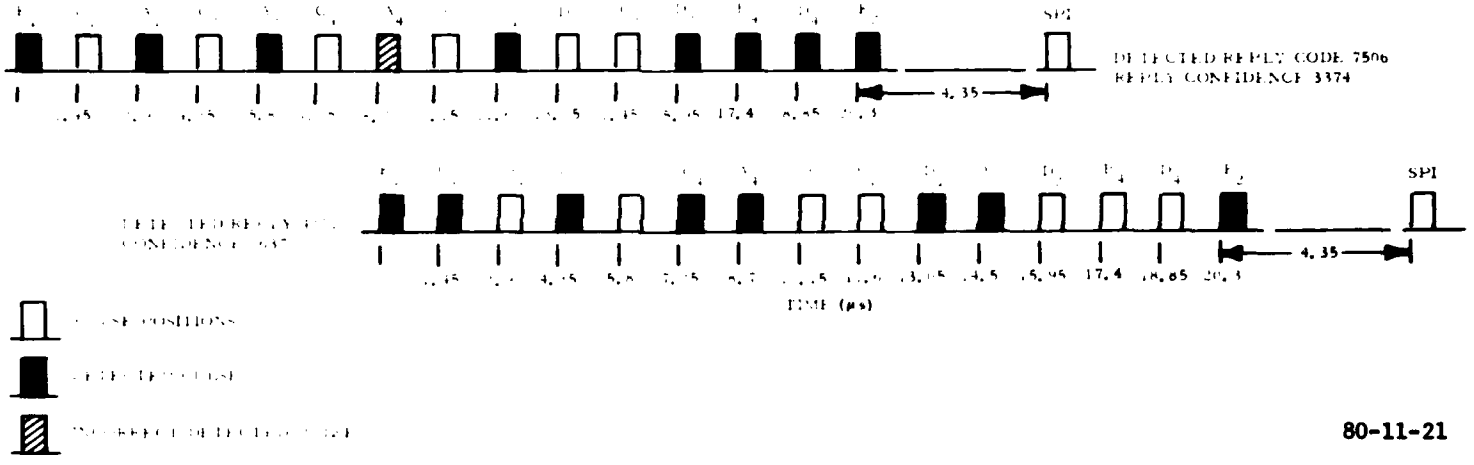

FIGURE 21. TEST REPLIES DECODED MONOPULSE DIFFERENCES OF 40, 20, AND 15

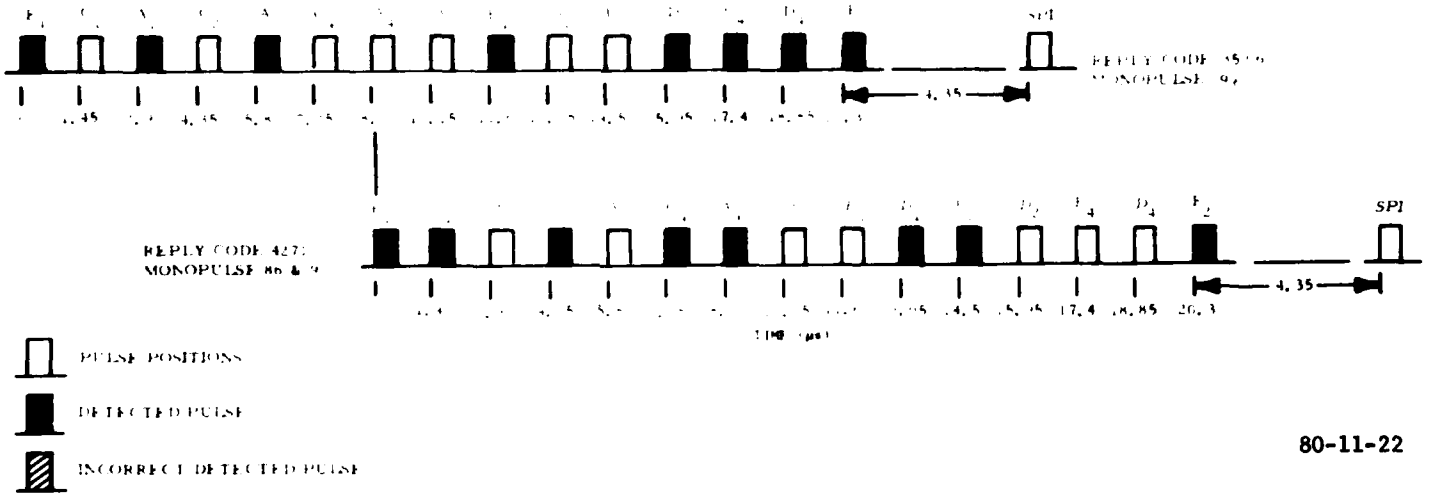

FIGURE 22. TEST GENERATED REPLIES MONOPULSE DIFFERENCES OF 10 AND 5

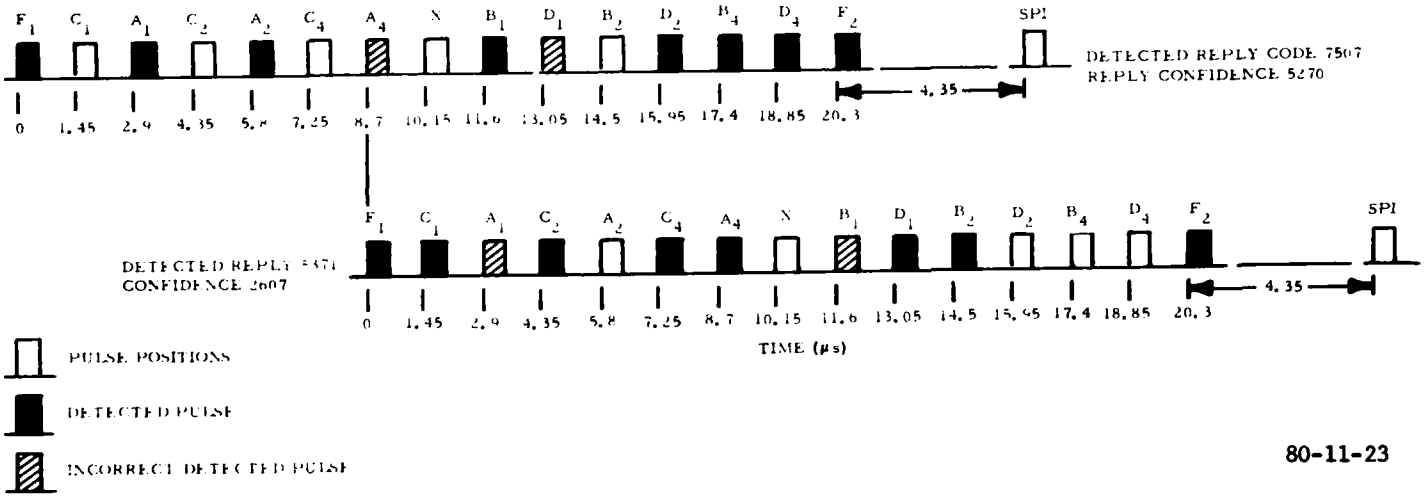

FIGURE 23. TEST REPLIES DECODED MONOPULSE DIFFERENCES OF 10 AND 5

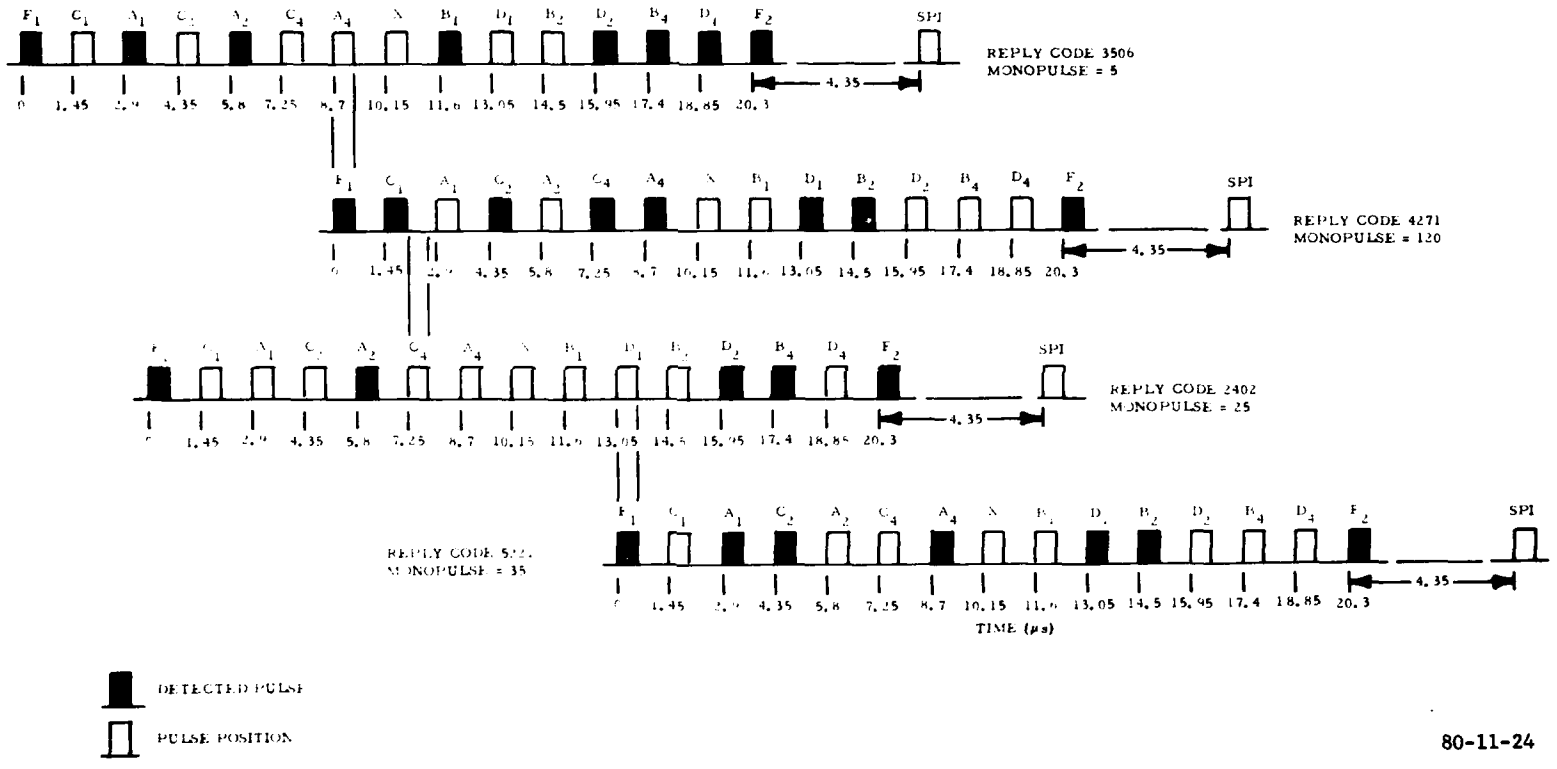

FIGURE 24. OVERLAPPED AND INTERLEAVED REPLIES

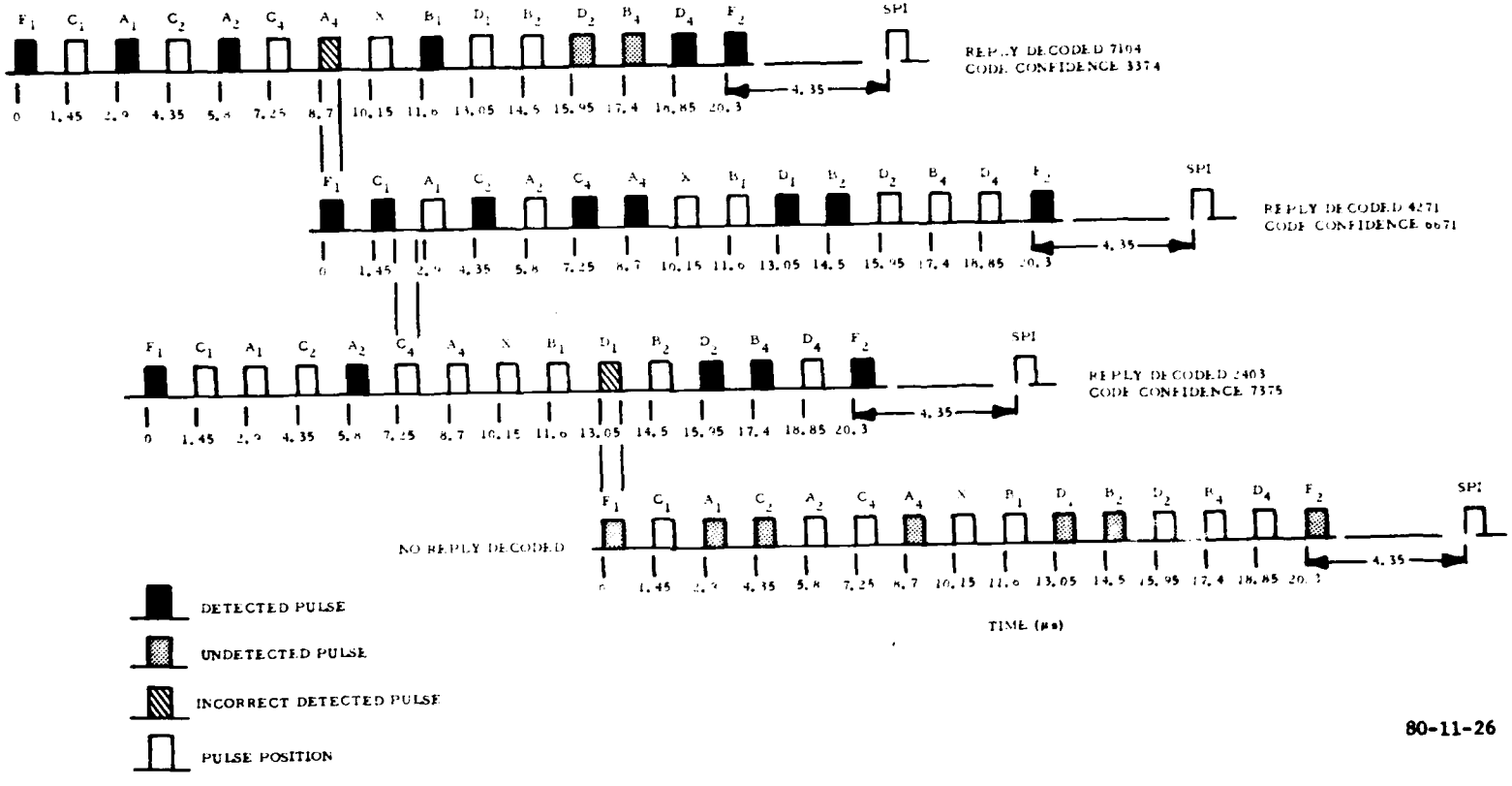

FIGURE 25. DECODED REPLIES FOR OVERLAPPED AND INTERLEAVED TEST SCENARIO

range and azimuth. Data were collected on magnetic tape for values of k equal to 5, 8, 10, and 15. The PDP-11/45 used two software data reduction programs to provide plots for each k value. Figure 26 graphically illustrates a "Monopulse Scatter Plot," where the y axis is the monopulse processor value, and the x axis is the corresponding off-boresight error in azimuth units (AU's). Figure 27 is a typical "Scatter Plot" of azimuth error in AU's versus off-boresight angle in degrees.

It was evident from a graphical analysis of all the plotted results for each k value, no measureable degradation of reply monopulse average estimates occurred.

TEST PROCEDURES AND RESULTS—PHASE III

DABS REPLY PROCESSOR PERFORMANCE EVALUATION.

These tests were designed to determine the performance of the critical elements of the DABS reply processor. The overall performance was measured with various input signal conditions and site-dependent adjustable parameters. The objective was to determine optimal values of two adjustable parameters, τ and G.

The parameter τ defined the number of valid pulses extracted from eight successive serial quantized sum data stream (SQΣD) samples. To be valid, a pulse must have been equal to logic 1. The parameter G determined the level of confidence of a reply. If the number of low confidence bits in any 24-bit span exceeded the value of G, the message was flagged as uncorrectable.

Testing was divided into two phases. Phase I determined the optimum adjustment of τ, to maximize the probability of preamble detection and minimize false preamble detect generation. Phase II determined the optimum adjustment of G, to provide the maximum probability of correct message decoding without producing undetected decoding errors.

PREAMBLE DETECTION (P_{pd}).

Two test configurations were implemented to collect data on processor performance. Phase I tests were accomplished using the configuration shown in figure 28. Basically, the DABS sensor was isolated from the real world environment to preclude external reply interference from entering the system. This configuration counted the number of preamble detects for various ATCRBS fruit levels. To insure that only valid detects were counted, the DABS preamble detector output was only declared when it occurred within a TTG generated test preamble window. The window was instituted prior to the preamble detect pulse. The number of false preamble detects was counted by enabling a test gate and disabling the test target generator All-Call reply.

Phase I testing involved a compromise between the probability of preamble detection and the probability of generating false preamble detects. A DABS preamble was declared when valid pulses were detected in all pulse positions of the preamble waveform, and at least two pulses had clear LE. Valid pulses were defined when at least τ out of eight successive samples of the SQΣD data stream were equal to logic 1.

Selected values of τ equal to 4, 5, 6, and 7 were tested for varying All-Call reply RF levels and for ATCRBS fruit levels of 1, 2, 4, 8, 16, 20, and 32,000 replies per second. Fruit was generated on a free running basis with random range, azimuth, and signal strength. Fruit was generated with a 10 percent main beam and a 90 percent side-lobe ratio.

A 100 percent preamble detection reference point was established for the simulated test target generator

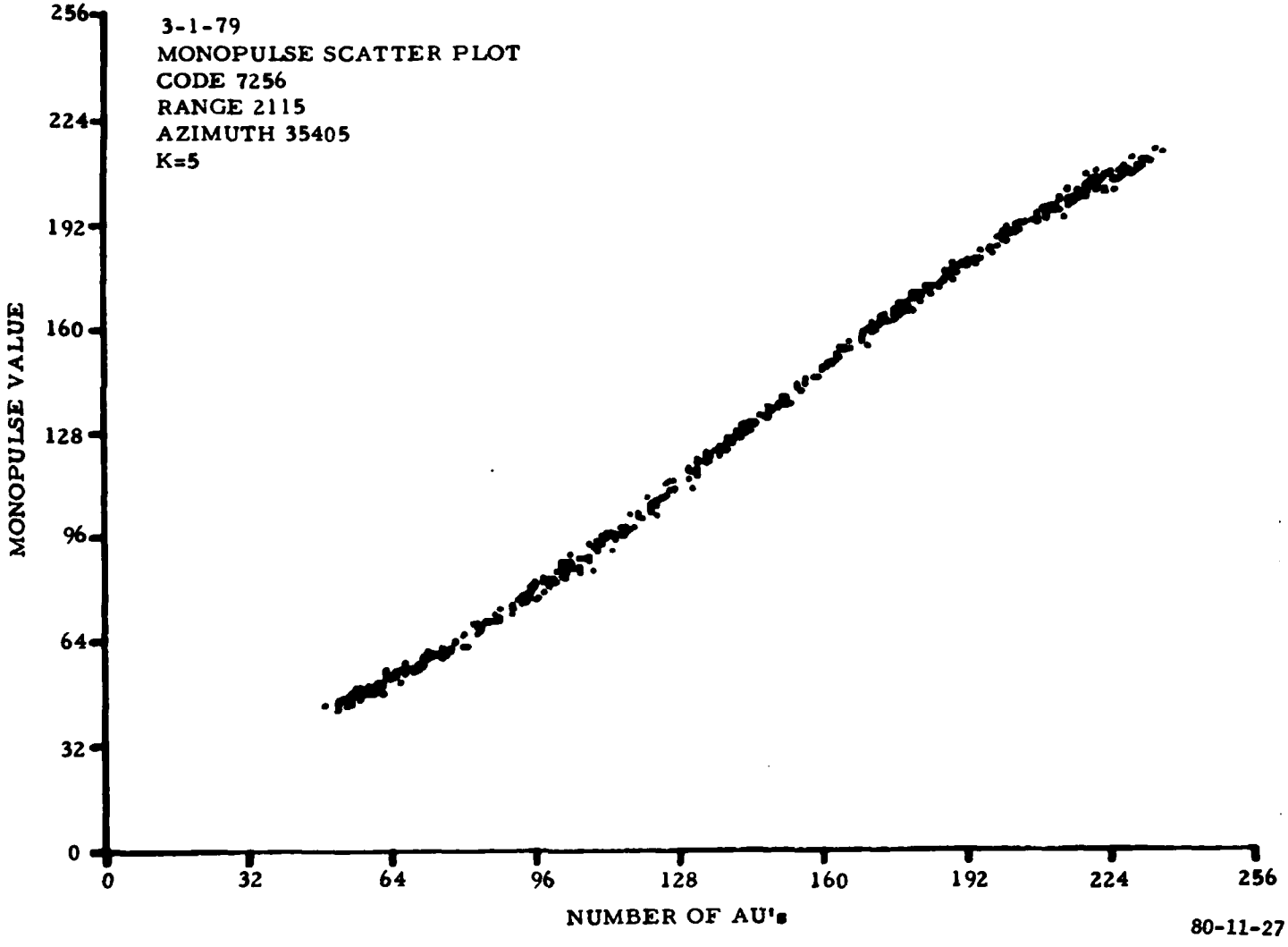

FIGURE 26. MONOPULSE SCATTER

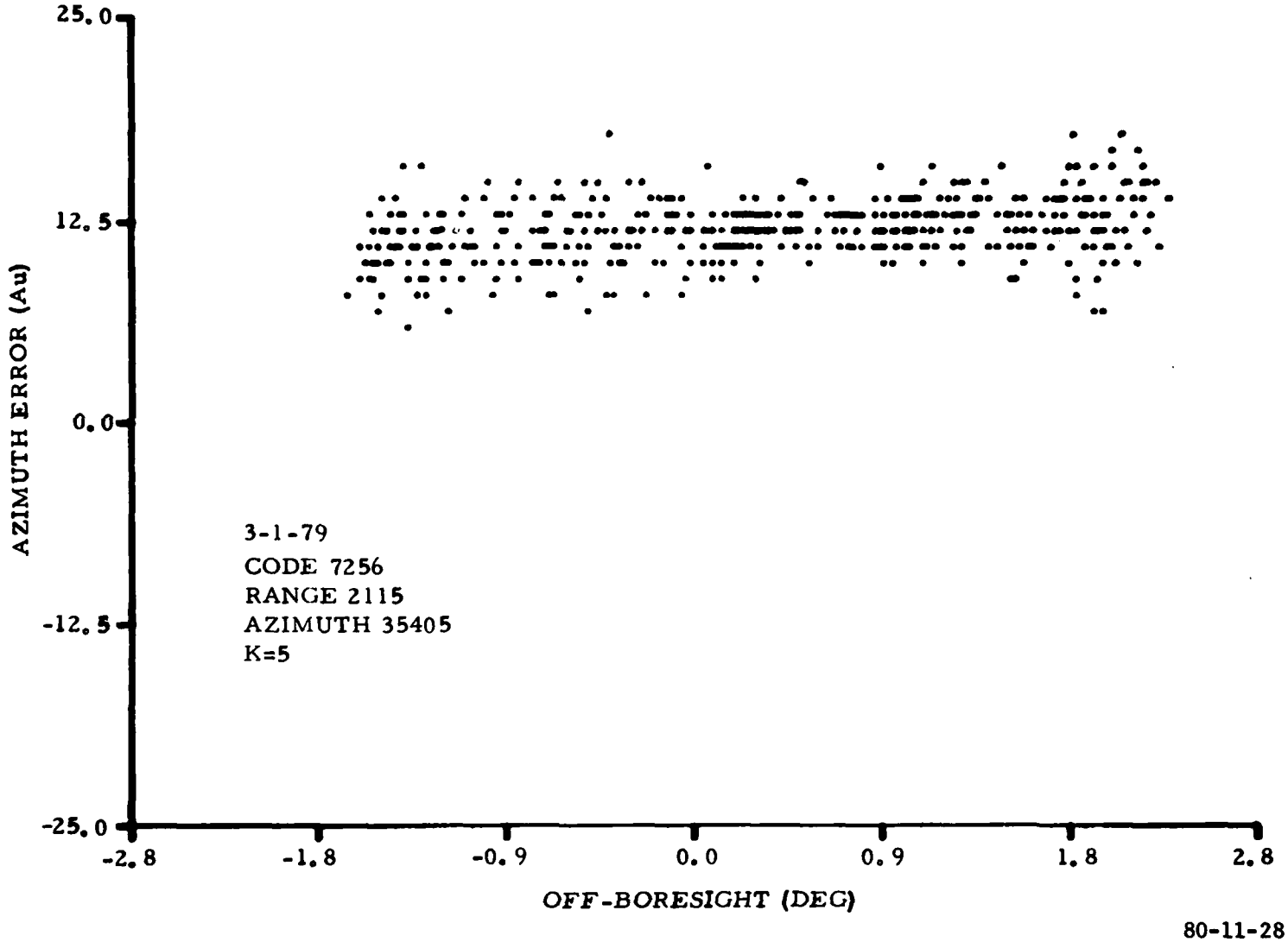

FIGURE 27. AZIMUTH ERROR VERSUS OFF-BORESIGHT ANGLE

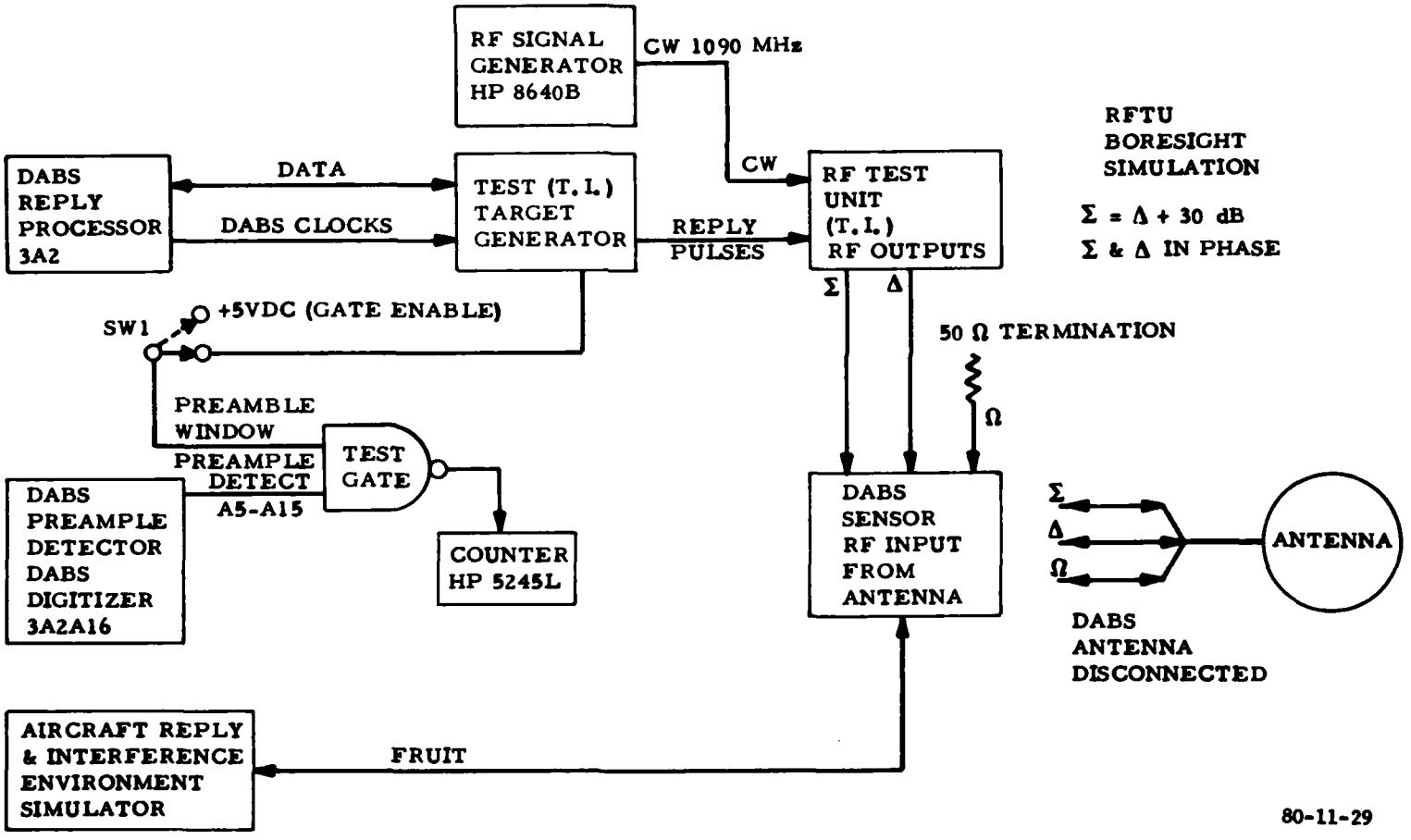

FIGURE 28. PREAMBLE DETECTION TEST CONFIGURATION

All-Call reply in a fruit free environment. This was accomplished by outputting the All-Call reply, via the RFTU, to the DABS sensor RF input port. The output of the preamble detector was used to trigger an electronic counter to indicate the presence of preamble detects. The RFTU's variable attenuator was manually adjusted when the count began to decrease. It was established that an RF test All-Call reply of -76 dBm at the sensor RF input port provided a preamble detection capability of 100 percent in the absence of all environmental fruit.

Measurements were made to determine the 90 percent preamble detection sensitivity. This was accomplished by attenuating the test target generators simulated preamble reply until the electronic counter displayed 90 percent of the established 100 percent reference count. It was established that an RF test preamble reply of -79.0 dBm at the sensor RF input port provided 90 percent bracket detection capability in the absence of all environmental fruit.

Tests were conducted for each selected τ parameter and test target generator All-Call replies. Each τ value was tested with ARIES simulated ATCRBS fruit. Reply signal strength was varied for each τ value and fruit level to determine reply sensitivity needed to provide 100 percent preamble detection. This was accomplished by decreasing the RFTU attenuation (equivalent to increasing signal strength) to obtain the same reference count on the electronic counter as for the All-Call reply without fruit.

The resulting reply signal strength for 100 percent preamble detection versus ATCRBS fruit levels as a function of the parameter τ are depicted in figure 29. These results indicate that reply sensitivity was reduced in the presence of increasingly large amounts of fruit. Analysis of the curves indicate that as τ increased (the number of samples out of eight which must be a "one"), percent preamble detection decreases.

FALSE PREAMBLE DETECTION (P_{fd}).

The probability of false preamble detections was determined during the preamble detection test. Detection of a false preamble was accomplished by disabling the test target generator and continuously enabling the test gate. When τ was set to values of 4 or 5, 100 percent preamble detection was achieved; however, the quantity of false detections increased. Optimal value for preamble detection and low false detection occurred when τ was equal to 6. When set to values of 5 and 6, 100 percent preamble detection was achieved without any false detections.

PROBABILITY OF CORRECT MESSAGE DECODING (P_{CD}).

Phase II testing involved establishing the optimum value parameter G. This parameter limited the number of undetected decoding errors by measuring low confidence bit density. Undetected decoding errors occur when: (1) the original errors in the received reply correspond to another valid reply producing a zero syndrome, and (2) a correctable bit pattern is produced by many bit errors generated in an uncorrectable pattern. When a correctable pattern is located by the error correcting logic, error correction occurs for error burst exceeding the 24-bit limit. In this situation, the uncorrectable message is corrected and the error becomes undetected. Tests were established to determine the influence G had on the probability of correct message decoding and establish its influence on undetected coding errors.

Testing was accomplished with the configuration shown in figure 30. The DABS diagnostic program for range, azimuth, and accuracy (RAA) was executed

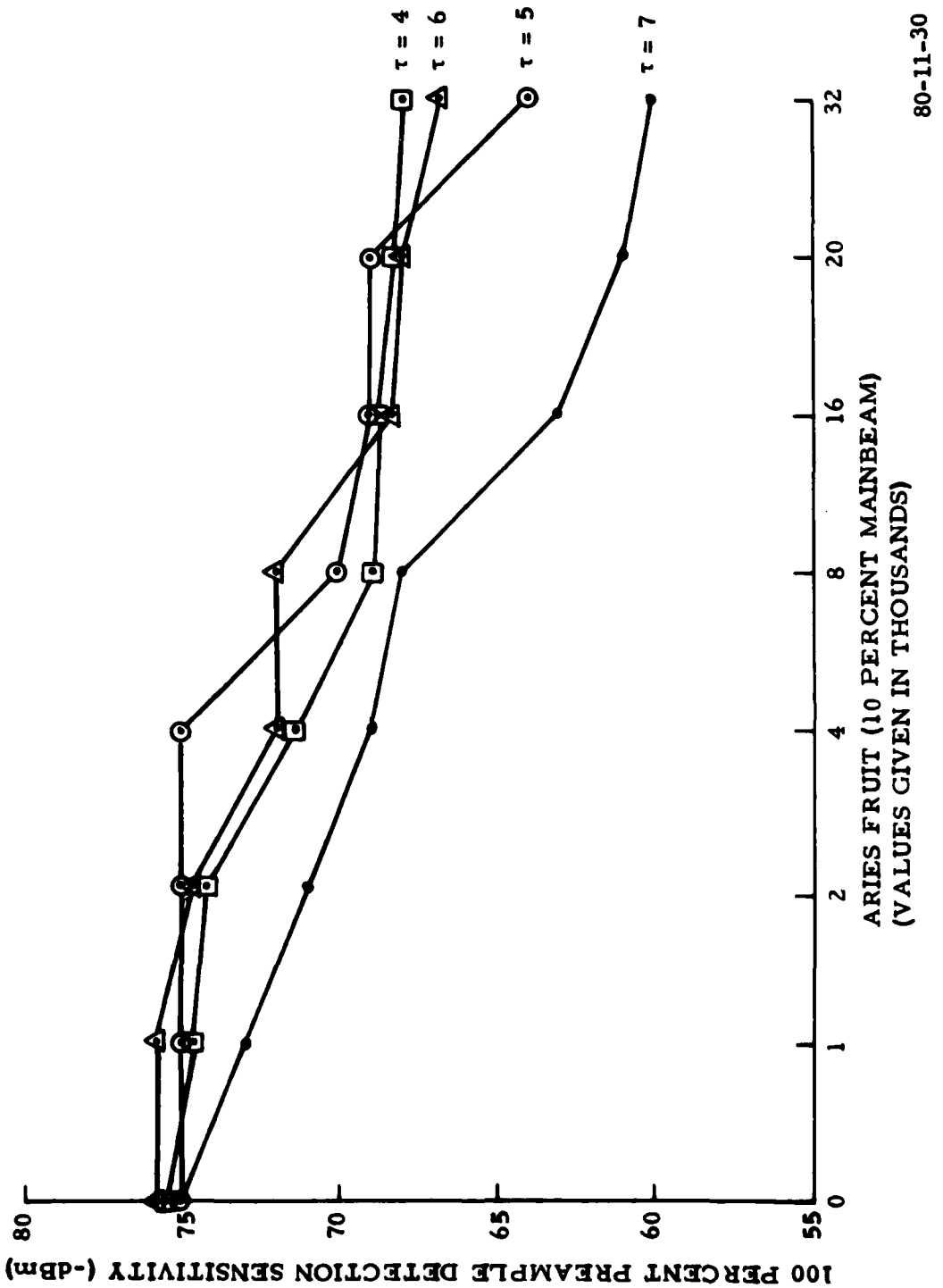

FIGURE 29. PREAMBLE DETECTION (P_{pd})

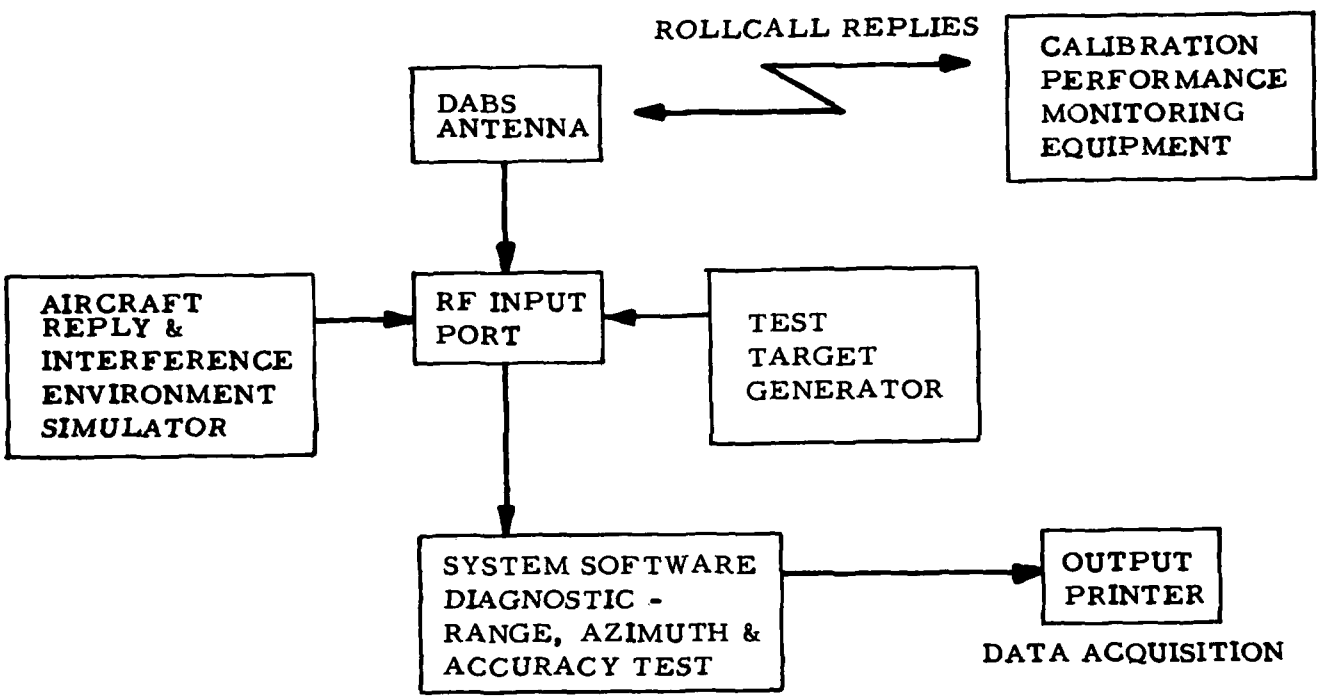

FIGURE 30. DABS MESSAGE BIT AND CONFIDENCE BIT ASSIGNMENT TEST CONFIGURATION

for data acquisition of roll-call replies. These replies were collected from the field located CPME. The CPME and RAA programs were used to eliminate the low pulse repetition frequency (PRF) of the transmitter. This would allow an increased rate of roll-call interrogations. Data were collected and plotted for two tests.

The first test was structured to determine the percent of correct message decoding as a function of G for various environmental ATCRBS fruit levels. The fruit was generated by ARIES on a free running basis with random range, azimuth, and signal strength. The fruit rate varied between 0 and 32,000 replies per second. Values of G equal to 9, 11, 14, 18, and 24 were tested.

The probability of correct decoding consisted of messages received without error and messages successfully corrected by the error correcting syndrome. Data were analyzed to establish the percent of correct message decoding, and the generation of undetected decoding errors resulting from the error correcting logic. The results are graphically presented in figure 31. The contribution made by the error correcting logic was represented by comparing the percent differences of correct decoding for various G values (figure 31). Correct messages were decoded at a rate of 98 percent for values of G equal to: 14, 11, and 9. Regardless of the value of G, degradation occurred for increasing values of ATCRBS fruit levels.

Undetected decoding errors were not observed during this phase of testing. The occurrence of undetected decoding errors for the fruit rates and system parameters tested was, as expected, a very low probability event.

No attempt was made to accurately measure the probability of undetected coding errors. A much more sophisticated data collection and analysis system capable of processing a large sample of DABS replies would be required to do so. It was sufficient to note that undetected decoding errors were not detected during any of the DABS message decoding tests.

The second test was also structured to optimize the parameter G. Testing was accomplished by overlapping test target generator ATCRBS replies with RAA CPME roll-call replies. Selected ATCRBS codes of 7700 and 7777 were chosen to represent light and heavy weight code density, respectively. Testing was performed for a variety of overlapped conditions. They were: overlapping of one, two, and three 7700 ATCRBS codes with the RAA CPME roll-call replies; and one, two, and three 7777 ATCRBS codes overlapped with the roll-call replies.

Data were collected and plotted as percentages of the correct message decoding which is a function of various parameter G values and ATCRBS code signal levels. Testing was performed for parameter G values of 24, 17, 13, and 11 for ATCRBS code signal levels of -10 dB, 0 dB, and +10 dB relative to the roll-call received signal level. The results are graphically presented in figures 32 through 37. The probability of correct decoding consisted of messages received without error and messages successfully corrected by the error syndrome. The collected data and plots were analyzed to establish the probability of correct decoding, probability of undetected decoding errors, and the contribution resulting from the error correcting hardware logic for the various values of G.

The contribution made by the error correcting hardware was represented by comparing the percent differences of correct decoding for the G values. All of the graphs depict an increased amount of degradation regardless of the value of G when the ATCRBS interferer-to-roll-call reply signal ratio became greater than one. The reason for this

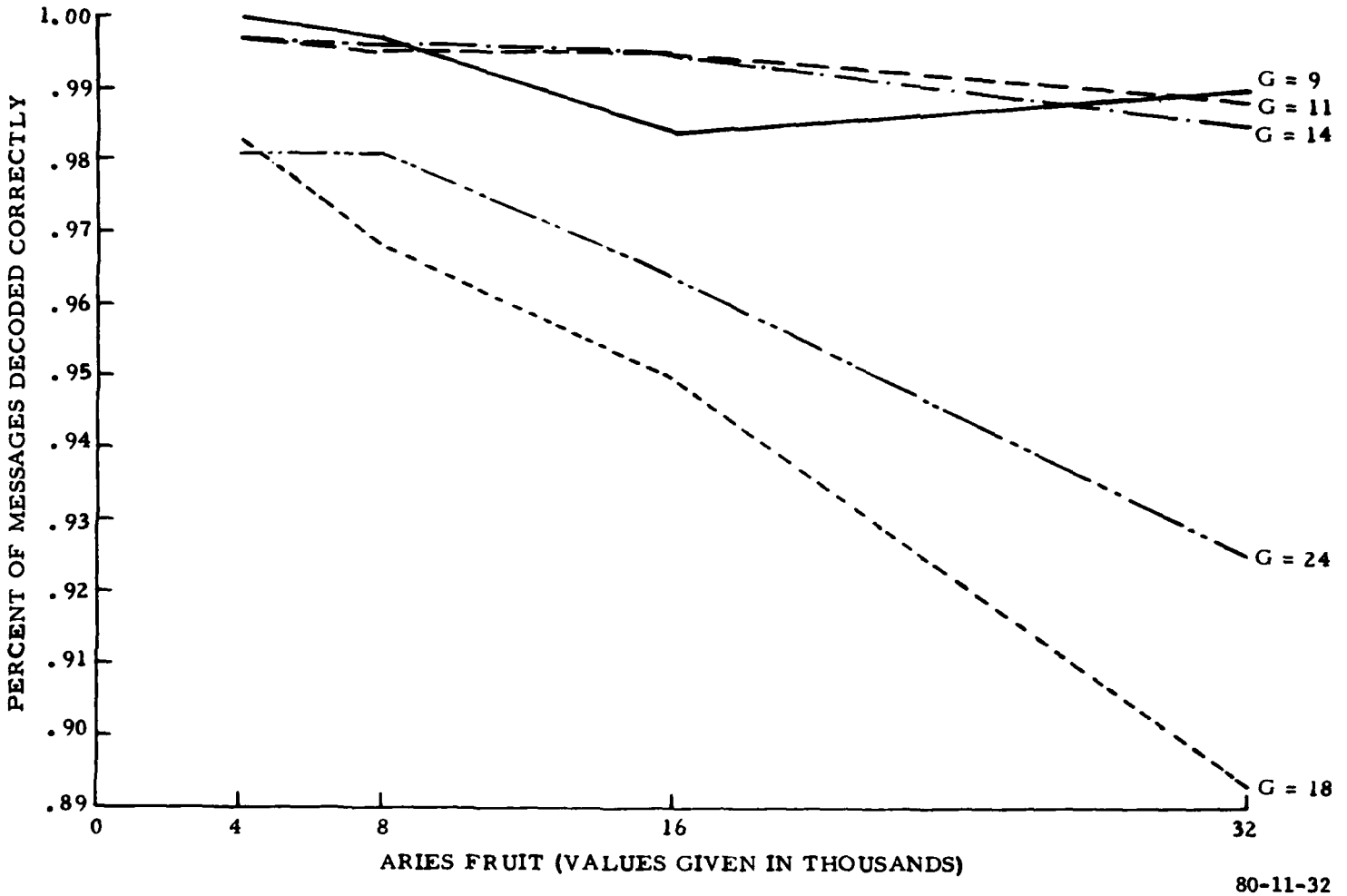

FIGURE 31. PROBABILITY OF CORRECT MESSAGE DECODING CORRECTLY (P_{CD})

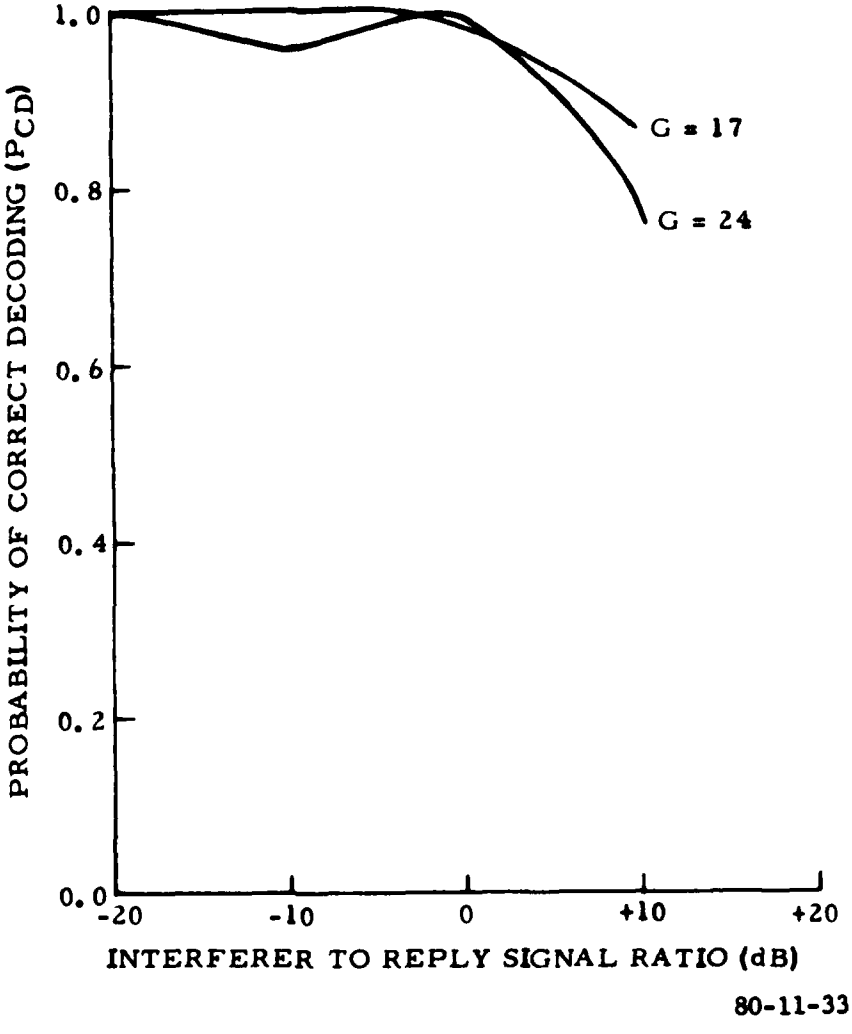

FIGURE 32. PROBABILITY OF CORRECT DECODING (P_{CD})—1 INTERFERER (CODE 7700)

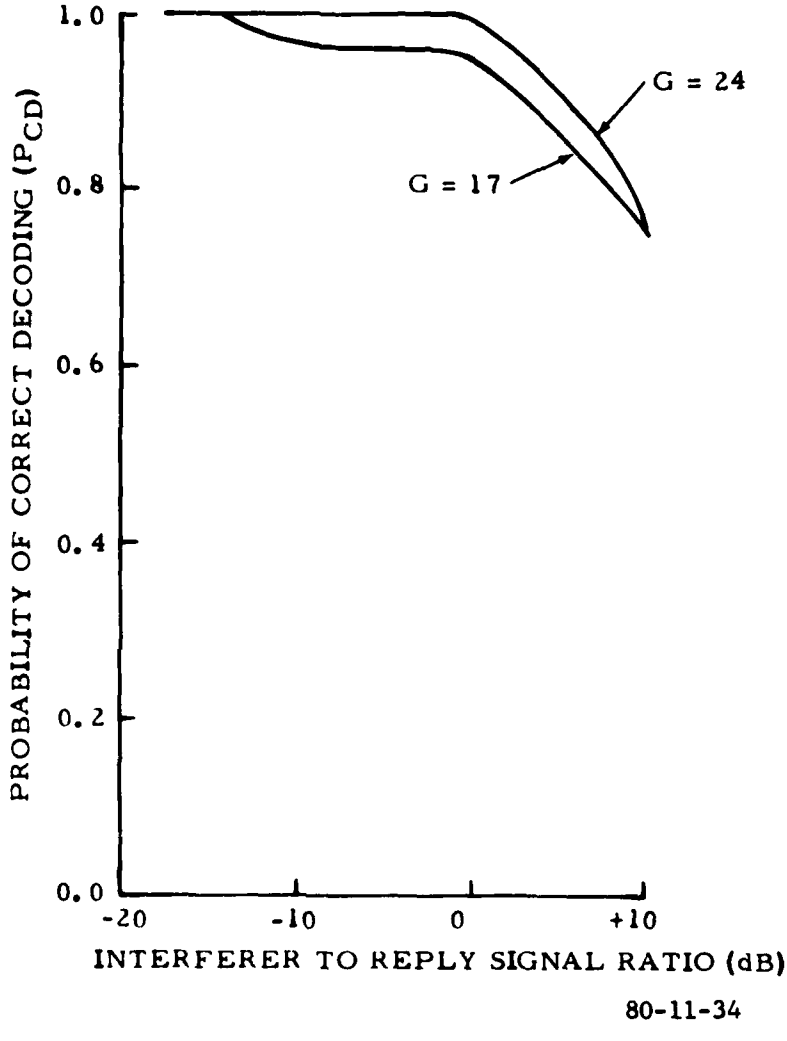

FIGURE 33. PROBABILITY OF CORRECT DECODING (P_{CD})—2 INTERFERERS (CODE 7700)

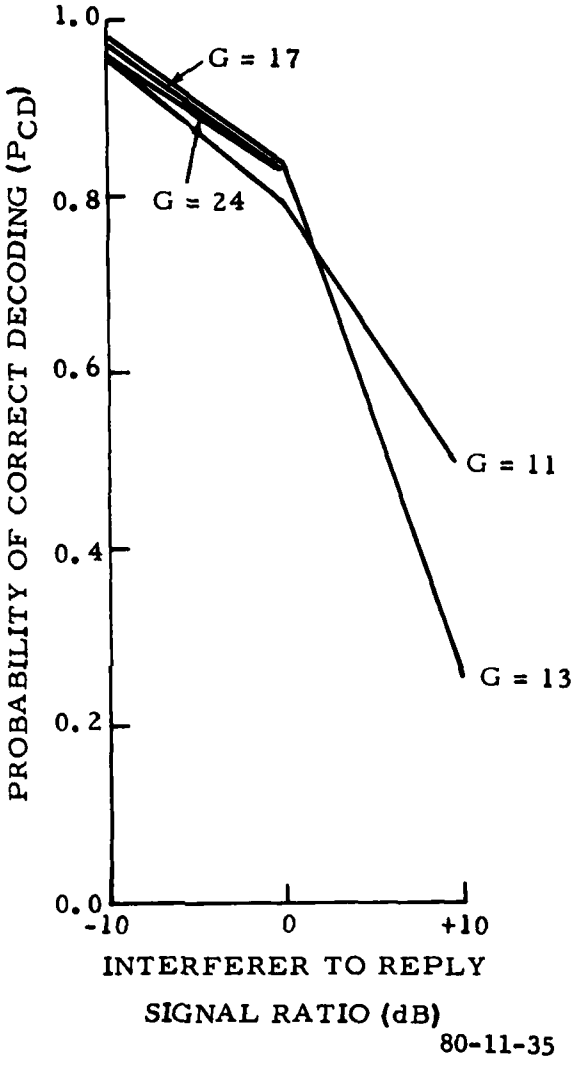

FIGURE 34. PROBABILITY OF CORRECT DECODING (P_{CD})—3 INTERFERERS (CODE 7700)

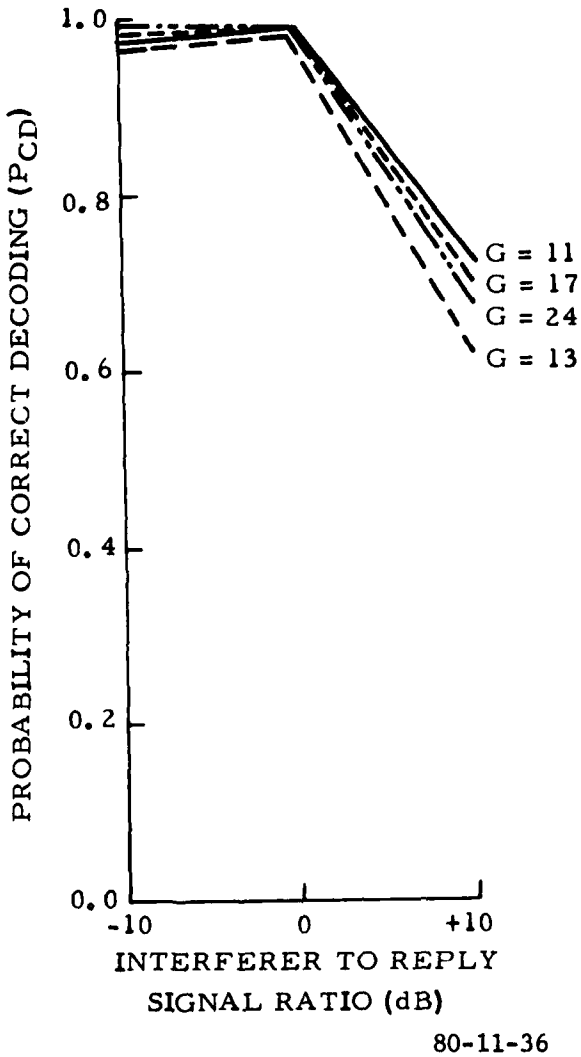

FIGURE 35. PROBABILITY OF CORRECT DECODING (P_{CD})—1 INTERFERER (CODE 7777)

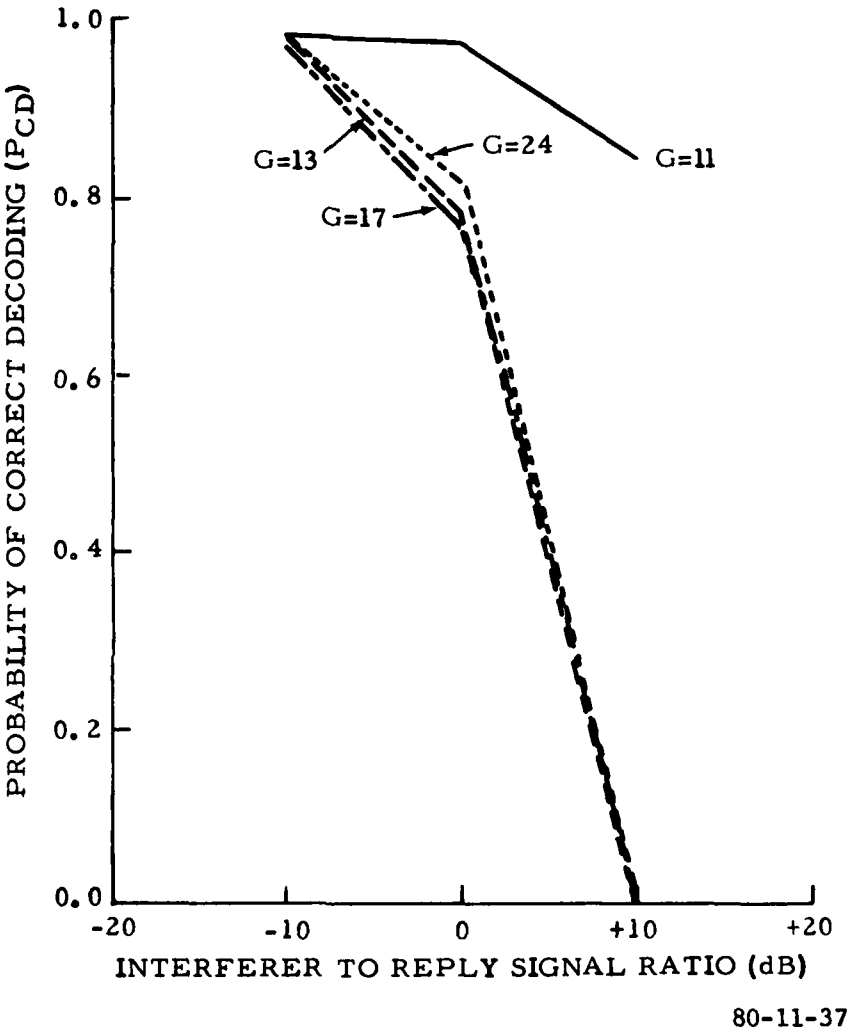

FIGURE 36. PROBABILITY OF CORRECT DECODING (P_{CD})—2 INTERFERERS (CODE 7777)

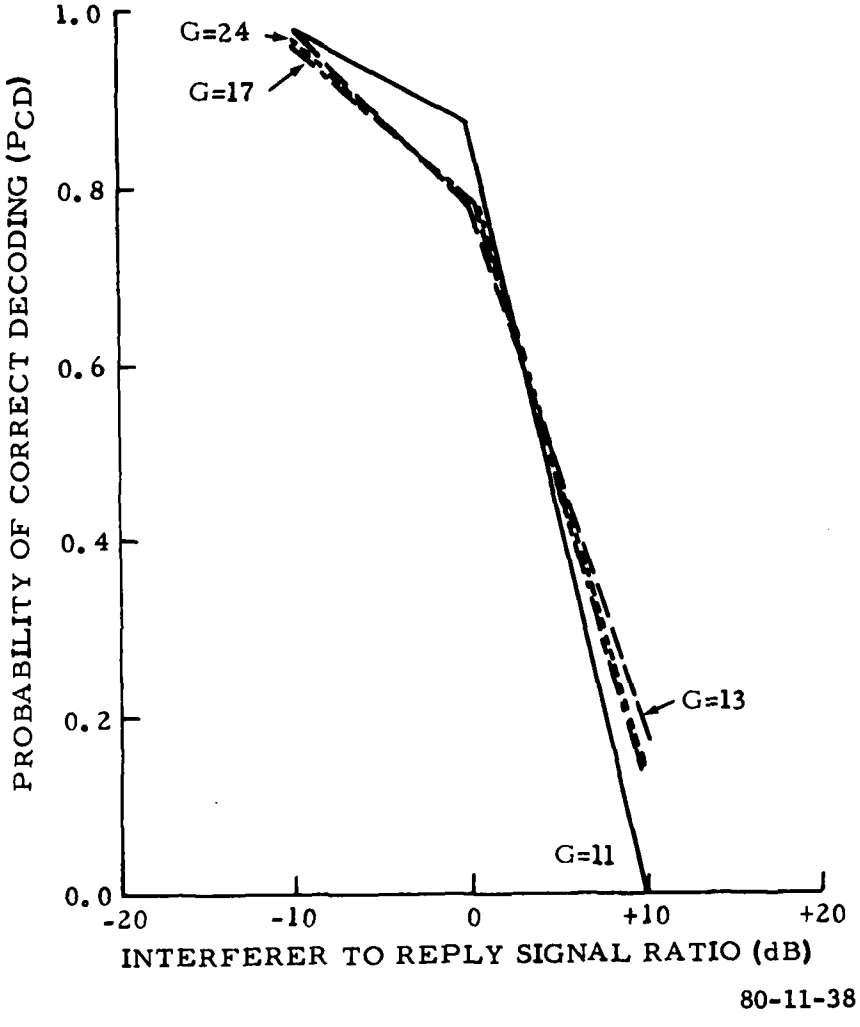

FIGURE 37. PROBABILITY OF CORRECT DECODING (P_{CD})—3 INTERFERERS (CODE 7777)

degradation was that more low confidence bits were being declared, requiring a lower value of G to allow additional error correction attempts. Analysis also revealed, that as the density of interferers increased, fewer messages were correctable for higher values of G. A value of G=11 represented an initial value large enough to benefit from the error-correcting capability. With reference to the figures, G=11 demonstrates the improvement which can be attained with the error correction code.

Undetected decoding errors did not occur for this test; therefore, a measure of the trade-off between the probability of correct decoding versus probability of undetected decoding errors as a function of G was not established. Because of this, a value of G=11 should be kept in perspective by remembering that there is a trade-off. This value is small enough to benefit from the error correcting code capability for one, two, and three ATCRBS interferers, and large enough to constrain the P_{UDE}.

CONCLUSIONS

Based on the results of the tests and evaluation (T&E) of the interrogation and processor (I&P) subsystem, it is concluded that:

1. The overall engineering requirement (ER) for the multichannel receiver is satisfactory. The log sum (Σ), difference (Δ), and omni (Ω) channels were found to track linearly to within ±1.0 decibel (dB) over the range -20 decibels above 1 millivolt (dBm) to -79 dBm. Monopulse accuracy was maintained over this dynamic range and over the frequency from 1087 to 1093 megahertz (MHz). The bandwidth frequency responses were flat to within ±0.1 dB and the differential amplitudes were within ±1.5 dB of each other. The difference/sum (Δ/Σ) peak-to-peak variation did not exceed $0.10\ (1+|\frac{\Delta}{\Sigma}|^2)$ for Δ/Σ ratios within calibration limits and the maximum variation from this calibration did not exceed $0.74\ (1+|\frac{\Delta}{\Sigma}|^2)$.

2. The leading and trailing edges, defined by quantized sum positive slope (QΣPS) and quantized sum negative slope (QΣNS) circuits, satisfactorily indicated when the slope of the Σ signal exceeded the preset threshold positive slope (T_{PS}) and threshold negative slope (T_{NS}) values. The adaptive threshold circuits suppressed low level multipath signals for K=25 dB and T=10 microseconds (μs). The quantized side-lobe suppression ATCRBS (QSLSA) and quantized side-lobe suppression DABS (QSLSD) successfully derived information which aided in determining the source of received replies within a designated sector of the antenna's beam width. The DABS fixed threshold parameter (T_{FD}) and the ATCRBS fixed threshold parameter (T_{FA}) were adjusted to +615 millivolts (mV). This provided 90 percent reply pulse detection at the sensor RF port for signal levels of -79 dBm. Maximum quantized sum DABS (QΣD) and quantized sum ATCRBS (QΣA) pulse detection occurred when threshold sum DABS ($T_{\Sigma D}$) 670 mV and threshold sum ATCRBS (T_A) 625 mV.

3. The Air Traffic Control Radar Beacon System (ATCRBS) video pulse quantizer correctly declares a pulse leading edge in the sum lead edge data stream when all of the following conditions were satisfied simultaneously: (1) $Q\Sigma A\ (t_1 + d) = 1$, (2) $Q\Sigma PS\ (t_1) = 1$, and (3) $Q\Sigma PS\ (t_1 + d) = 0$. Pseudo-leading edges were correctly inserted in the ΣLE data stream for wide pulses and rejected for narrow pulses.

4. Bracket detection in the absence of all fruit replies was 100 percent for two pulses having signal levels of -20 dBm and spaced 168 ±1 sample intervals (20.3 ±1 μs) in the ΣLE data stream. Ninety-eight percent detection was achieved with two -50 dBm

pulses with fruit levels up to 32,000 replies per second, and 60 percent at -70 dBm and 32,000 replies per second. Ninety percent detection was achieved at -79 dBm at the sensor radiofrequency (RF) port in the absence of all fruit replies. This performance is considered acceptable to support detection of ATCRBS targets.

5. The pulse processing and code confidence bit assignment rules stipulated in Federal Aviation Administration (FAA) engineering requirement (ER) FAA-ER-240-26, for both clear and overlapped pulse positions, are followed.

6. The ATCRBS monopulse correlation constant k provided optimum reply decoding performance when adjusted to 10; no measureable degradation occurred in reply monopulse average estimate when adjusted to 5, 8, 10, or 15.

7. Incorrect code information occurred when the first bracket pulse of one reply corresponded to an unused code information position of a previous reply. This condition resulted in a code pulse declaration for the unused code pulse position of the first reply with an assignment of low confidence. This effect occurs for cases where the monopulse value for the two reply trains is different enough to allow proper pulse association. The result was the detection of both replies, but only correct code pulse information for the code train farthest in range. This was due to a subtle flaw in the DABS engineering model specification which has been corrected in FAA-ER-240-26A.

8. Ninety percent preamble detection (P_{pd}) was achieved at -79 dBm at the sensor RF port in the absence of all fruit replies.

9. As the preamble valid pulse parameter (τ) increased, more preambles are undetected. A decrease in τ increases false preamble detection in the presence of ATCRBS fruit. The optimal value for preamble detection in a 0 to 32,000 fruit replies per second environment occurs when τ equals 6.

10. Message degradation increases regardless of the value of G employed as the signal interferer to reply ratio exceeds 1. As the density of ATCRBS interferers increase, fewer messages are correctable for larger values of G. A value of G=11 represents an initial value large enough to obtain the error correcting capability, with respect to interferers, without increasing the high rate of undetected errors.

11. DABS message bit processing and confidence bit assignment is in agreement with the ER bit processing decision rules.

RECOMMENDATIONS

It is recommended that:

1. The quantized sum slope threshold parameters (T_{PS} and T_{NS}) initially be adjusted to -149 millivolts (mV) and +149 mV, respectively.

2. The omnithreshold parameter (T_{Ω}) initially be adjusted to +750 mV and the difference threshold parameter (T_{Δ}) initially be adjusted to -300 mV.

3. To reduce the likelihood of detecting low-level multipath signals as reply pulses, operate the Discrete Address Beacon System (DABS) and Air Traffic Control Radar Beacon System (ATCRBS) adaptive thresholds (T_{ADAPA} and T_{ADAPD}) at K=25 decibels (dB) and T=10.0 microseconds (μs).

4. Both the DABS and ATCRBS fixed threshold parameters (T_{FD} and T_{FA}) be adjusted to +165 mV to attain 90 percent reply detection for signal levels at -79 decibels above 1 milliwatt (dBm) at the sensor radiofrequency (RF) port.

5. The ATCRBS monopulse correlation parameter be adjusted to k=10 to attain optimum reply decoding.

6. Initially, the DABS preamble valid pulse parameter (number of successive samples of each preamble pulse valid) be adjusted to $\tau = 6$.

7. The DABS confidence test parameter be adjusted to G=11.

8. Reevaluate the digital ATCRBS processor hardware in the production model of DABS to confirm that the changes to Federal Aviation Administration (FAA) engineering requirement (ER) FAA-ER-245-26A pulse processing rules corrected the improper insertion of the F_1 or F_2 pulses in a reply code train.

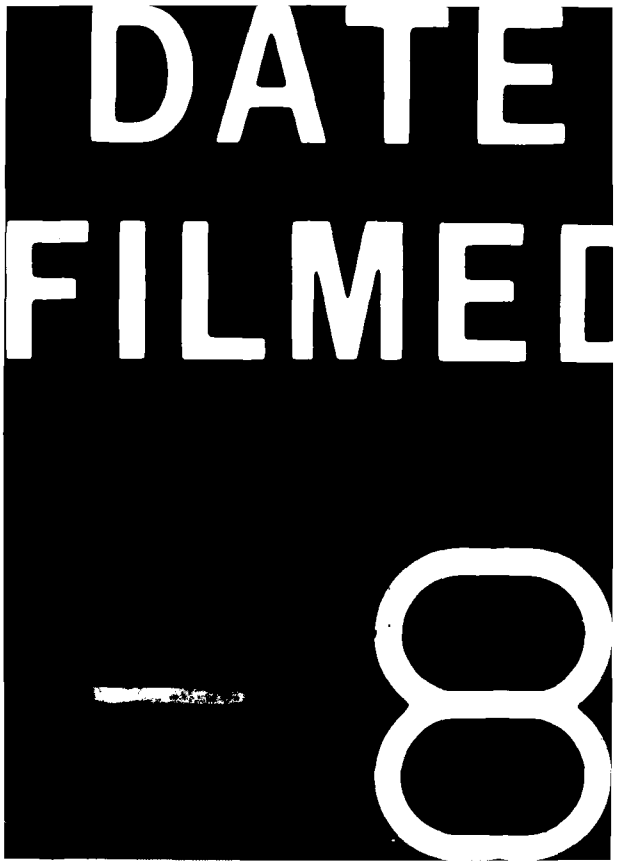
DATE
FILMED
8